

X-513-65-225

FACILITY FORM 602

~~N 66~~ 11199

(ACCESSION NUMBER)

39
(PAGES)

(THRU)

1
(CODE)

(NASA CR OR TMX OR AD NUMBER)

07
(CATEGORY)

NASA TM X-55303

APOLLO ENTRY RADAR ACQUISITION STUDY

BY
JAMES R. MOORE

GPO PRICE \$ _____

CFSTI PRICE(S) \$ _____

Hard copy (HC) 2.00

Microfiche (MF) .50

ff 653 July 65

MAY 28, 1965



— GODDARD SPACE FLIGHT CENTER —
GREENBELT, MARYLAND

APOLLO ENTRY
RADAR ACQUISITION STUDY

by

J. R. Moore
Systems Analysis Office

Goddard Space Flight Center
Greenbelt, Maryland

TABLE OF CONTENTS

	<u>Page</u>
INTRODUCTION	1
I. TRAJECTORY INFORMATION	2
II. SEARCH SECTOR	3
III. TARGET CHARACTERISTICS	4
IV. RADAR CHARACTERISTICS	6
V. PROBABILITY OF ACQUISITION	6
VI. CONCLUSIONS	8
ACKNOWLEDGMENT	9
REFERENCES	10

APOLLO ENTRY RADAR ACQUISITION STUDY

SUMMARY

It is desired to evaluate the effectiveness of an active earth-based radar against a target as represented by the Apollo Command Module during the re-entry phase of the mission. The radar is to be used for acquisition of the Command Module, and for tracking during the ionization blackout. It can also serve as a backup for acquisition and tracking in case of failure of the on-board transmitting facilities.

As presently proposed, the radar for use in connection with the Apollo equipment would have new transmitting and receiving equipment sharing a modified version of the present antenna with the "S" Band CW equipment. Dr. F.O. Vonbun has proposed that the system be simplified by adding a pulse mode to the present transmitting and receiving equipment with the necessary modifications to the antenna assembly.

As proposed, the radar must be frequency displaced from the S-Band CW equipment and cannot utilize the present transponder. Radar operation is limited to skin tracking or tracking of the ion sheath.

Trajectories have been studied to determine the position, velocity and aspect angles of the module relative to a number of proposed station locations.

The radar has been assigned a search raster, six degrees high by twenty-three degrees wide. The radar must search this raster in a five second period with a 50 percent probability of acquisition on a target of one square meter at a range of 281 nautical miles.

It has been found that, when the station is positioned on the projected ground track of the trajectory at a distance of about 850 miles from the re-entry point, the probability of detection is better than 99.9 percent for all normal trajectories.

Since, in many trajectories, the ionization sheath extends beyond the station location, the radar should have overhead tracking capability. It should also have sufficient angular accuracy to insure S-Band lock-on at the termination of the blackout period.

APOLLO ENTRY RADAR ACQUISITION STUDY

INTRODUCTION

It is desired to evaluate the effectiveness of an earth-based active radar for acquisition and tracking of the Apollo Command Module during the re-entry phase of the mission.

To implement the study, information has been accumulated relative to the trajectory of the module during the re-entry. An effort has been made to select normal trajectories which provide the greatest lateral or vertical dispersion during the early part (first 800 nautical miles) of the re-entry phase. A normal trajectory is defined as a trajectory which enters at an angle between -5.53° and -7.51° and which does not exceed the 10g total acceleration limitation for a sustained period during this part of the trajectory.

From the trajectories, the position and velocity of the module are established in time. Also, the angle between the velocity vector and the line of sight from the module to the tracking station may be ascertained. This angle may be added to the module angle of attack to give the maximum aspect angle between the module axis and the line of sight to the station.

It is shown that the radar target size presented by the module depends upon the aspect angle. Thus, when the aspect angle is known or bounded, the size of the radar target is known.

It has been assumed that the radar will search a window which is 23° wide and 6° high. The window will be scanned in a period of five seconds. The radar will have a 50 percent probability of detection and acquisition on a one square meter target at a range of 281 nautical miles for each scan of the window.

An examination of the vertical and horizontal projection of the trajectory data has shown that the window should be elevated to an angle of seven degrees above the horizon for near optimum performance. That is, with a maximum operating range of 281 nautical miles, the center of the window should be seven degrees above the horizon.

Since, as far as we now know, horizontal dispersions may be either left or right, the station should be located on the projected ground track of the approach trajectory.

Detection probabilities and other performance parameters have been computed for stations located between 600 nautical miles and 1,100 nautical miles from the re-entry point. The merits of the various station positions are discussed in the following.

I. TRAJECTORY INFORMATION

Numerous trajectory studies have been made in this Office^{1,2} and in other agencies. These studies are concerned with the position and velocity of the module after contact with the atmosphere at an elevation of 400,000 feet above the surface of the earth. At the present time, trajectories during re-entry are based upon equations developed by Dean R. Chapman³ and implemented in a proposed guidance system by J. P. Bryant and M. P. Frank.⁴

At the present time, trajectories with entrance angles between -5.53° and -7.51° are still considered feasible. The design entrance angle, and most probable, is -6.00° . Although ground track re-entry ranges between 1,500 and 5,000 nautical miles are still possible, the region between 1,500 and 2,500 nautical miles is favored.

Vertical projections, for the design entrance angle are shown in the first three figures. Figure 1 is for a 1,500 mile longitudinal ground track, Figure 2 is for a 2,000 mile path, and Figure 3 is for a 2,500 path.

The initial portions of two trajectories are shown in Figure 4. It can be seen from this figure that small changes in the lift to drag ratio, in the proximity of the current 0.35 design value, induce only minor changes in the normal trajectory, provided other parameters are not changed.

The early part of the re-entry trajectory, which is the primary concern during acquisition, is influenced by the entrance angle. Figure 5 is the vertical projection of 2,000 nautical mile normal trajectories having different entrance angles. As indicated, the first minimum altitude point is dependent upon the entrance angle.

Although this report is based upon a fixed vertical elevation angle for the window for all trajectories, some improvement could be obtained by a slight change in the elevation angle to match the entrance angle when prior knowledge of the entrance angle is available.

The horizontal projection of the early portion of the re-entry trajectory is shown in Figure 6 for a number of representative conditions. Since horizontal dispersion beyond the window of the radar is the most serious limitation to down-range placement of the station, effort has been extended to obtain the normal trajectory with the maximum lateral range. It is unlikely that a trajectory with maximum lateral range would be deliberately flown. Curve A of Figure 6, a short trajectory with near design entrance angle, gave the maximum possible lateral displacement under normal trajectory constraints, and has been used for estimating horizontal aspect angles for this report.

The influence of ionization induced by the high velocity of the module thru the atmosphere is being studied in this Office and other agencies. It is shown in NASA Technical Note TN-D-2732⁵ that the limits which bound the blackout region are functions of the altitude, the velocity and the frequency of transmission. The blackout limits as given in Reference 5 are spotted in the trajectories for a radio frequency of two-thousand two-hundred megacycles corresponding to S-Band.

The possibility of a precursor blackout of reflected signals has been pointed out by R. L. Daniels of North American Aviation, Inc. in the "Final Report on Apollo Plasma Re-Entry Studies."⁶ The estimated position of such an absorption band is given as extending from 200 nautical miles to 370 nautical miles from the point of re-entry. A second absorption band is also predicted in the proximity of the second entry from the skip-out type trajectory.

Although the precursory absorption bands have not been proven in any experiment, they will be taken into consideration in the selection of an optimum position for the ship. Figure 7 shows the location of the possible precursor attenuation band in the early re-entry trajectory.

II. SEARCH SECTOR

It is anticipated that the position and velocity of the Command Module will be well known at the initial point of re-entry (defined as an elevation of 400,000 feet above sea level, see Reference 1 Figure 14. After contact with the atmosphere, the module is subject to aerodynamic lift and drag, so that departure from the initial trajectory may increase with time. Thus, the earlier acquisition can be established and maintained by the ground station, the smaller will be the mandatory search sector.

A number of factors favor a delayed acquisition, As mentioned before, an absorption area resulting from precursory blackout should be avoided. Also, it

is desired to take telemetry data for a maximum time and a down track position will afford longer post-blackout communication time. The possibility of sustained communications is improved by delaying acquisition until after the initial transient trajectory gyrations have subsided.

However, if the station is located too far from the re-entry point, an erroneous maneuver, possible during the initial phase of the re-entry program, could preclude the possibility of acquisition.

After reviewing the Re-Entry Trajectories described in Reference 1, the Manned Flight Support Office proposed a solid angle sector six degrees high by 23° wide as being suitable for initial investigations with search radar. This window has been used for computations in this study with quite satisfactory results.

The desired threshold detection range was proposed as 500 nautical miles with a range of 250 nautical miles listed as suitable. The search sector is shown in Figure 8.

III. TARGET CHARACTERISTIC

Computations for the radar cross-section of the Command Module have been made in the Final Report on Apollo Plasma Re-Entry Studies, (Reference 6). Figure 11 on Page 22 of the referenced report is repeated as Figure 9 in this report. For this report, a conservative target size is desired. Since there is some question as to the gain afforded by the plasma sheath, the increase in target area between zero and 15° , and between 35° and 52° on Figure 9 will be ignored. Also, since the sheath can be detrimental, the derogatory effect of the plasma between 15 degrees and 32 degrees will be included. The resultant target size is shown in Figure 10.

The target size selected includes the degradation due to absorption, and degradation due to ablator material in the forward hemisphere.

The angle of attack, that is the angle between the axis of the module and the velocity vector is assumed to be constant at 23° . However, the direction of the lift vector is determined by the roll angle of the module, and since lift may be desired in any direction, the roll angle is not known. In order to include the most unfavorable conditions, the angle of attack is assumed to be 23° at the most unfavorable roll angle. Thus, the aspect angle will be 23° plus the angle between the velocity vector and the radius vector from the module to the radar.

The angle between the velocity vector and the radius vector from the module to the radar may be determined from the trajectory. Since each trajectory is different, the angles vary with the trajectory parameters. This angle, which will be called the trajectory angle, is plotted against station position in Figure 11 for a trajectory which passes directly over the station with no lateral deviation. These angles are taken from the 5,000 mile trajectory. Shorter trajectories yield slightly smaller, and consequently more favorable trajectory angles. Figure 12 is a plot of the horizontal projection of the trajectory angles for a trajectory with maximum lateral displacement. These angles apply to a 1,500 mile normal trajectory, which trajectory yields the largest and most unfavorable horizontal trajectory angles.

It should be observed that there is very little deviation with trajectory length for either the vertical or horizontal trajectory angles.

As indicated previously, the aspect angle is the sum of the trajectory angle and the angle of attack. In the limiting situation, the aspect angle may be determined by adding 23° to the trajectory angle.

Figure 13 is a plot of the vertical aspect angles against the station positions, and Figure 14 is a plot of the projection of the maximum horizontal aspect angles as computed from the trajectory angles in Figures 11 and 12.

By comparing the possible aspect angles, Figures 13 and 14, with the radar target size, Figure 10, it can be seen that in the limiting condition the target size will be one square meter or larger for the portion of the trajectory under consideration during acquisition. Consequently, in the interests of conservative computations, a target size of one square meter has been selected for the analysis of the radar capability.

The aspect angle is determined largely by the roll angle. It is quite possible for the module to pass through the acquisition beam with an aspect angle less than 30° during the entire transit. Thus, the target size could be 10 square meters or more during the acquisition phase.

The velocity of the module during the early part of the re-entry phase has been computed by the relations developed in Reference 3 and 4. Figure 15 is a plot of the velocity for four characteristic trajectories, in feet per second. The velocities are plotted in miles per second in Figure 16.

IV. RADAR CHARACTERISTICS

For the purpose of this analysis, only the overall performance of the radar need be specified. It is assumed that the radar will be capable of transversing the 6° by 23° search sector in a five second period. The probability of detection for one five second search is to be 50 percent on a 10 square meter target at a range of 500 nautical miles. The range for the same detection probability on a one square meter target will be 281 nautical miles.

Automatic target recognition is assumed. The rate of false targets must be kept to a reasonable minimum, and provisions should be incorporated to automatically dispense with false alarms. In the calculations, a false alarm probability of 10^{-6} was used.⁸

Other radar characteristics will be specified by other phases of the mission (tracking, etc.) and need not be considered at this time.

V. PROBABILITY OF ACQUISITION

After examination of a number of trajectories, it has been found that an angular elevation of seven degrees above the horizon (to the center of the search sector) is about correct for optimum performance on the majority of the trajectories. With prior knowledge of the entrance angle and the exact re-entry point, a different elevation angle may yield slightly better results. However, in view of possible deviations from planned flight paths, a location and elevation which gives good acquisition over all possible trajectories is considered most desirable. For these initial computations the fixed elevation angle of seven degrees is used for all station positions.

The station is located on the extension of the pre-re-entry trajectory with the vertical center line of the window in the plane of the pre-re-entry trajectory.

Four trajectories have been selected for probability studies. These trajectories have been selected to include the average and extreme normal conditions. Those selected are the following:

(a) Longitudinal Distance	= 5,000 nautical miles
Lift-to-Drag Ratio	= 0.4
Entrance Angle	= -6.0°
Maximum Lateral Distance	

(b) Longitudinal Distance	= 1,500 nautical miles
Lift-to-Drag Ratio	= 0.4
Entrance Angle	= -6.0°
Maximum Lateral Distance	
(c) Longitudinal Distance	= 2,000 n. mi.
Lift-to-Drag Ratio	= 0.4
Entrance Angle	= -7.51°
Maximum Lateral Distance	
(d) Longitudinal Distance	= 2,000 n. mi.
Lift-to-Drag Ratio	= 0.4
Entrance Angle	= -5.53°
Maximum Lateral Distance	

Information pertinent to trajectory (a) has been tabulated in Table 1. As indicated, the distance traveled in the radar window is a maximum when the station, or ship, is 700 nautical miles from the re-entry point. Distance traveled in the acquisition beam is plotted for this, and the other trajectories, in Figure 17. However, since the velocity is decreasing, as shown in Figure 16, the time available for acquisition increases with ship position to a distance of 925 nautical miles from the re-entry point. Time available for acquisition is plotted in Figure 18.

Based upon the range corresponding to the starting point of each five second interval, the probability of detection during that interval has been computed.⁸ The probability of detection and acquisition for trajectory (a) has been plotted for each five second interval in Figure 19. There is a curve for each ship location. It should be observed that this plot is for the detection probability for each individual interval, not the accumulated probability over the trajectory.

Similar data for trajectories are tabulated in Table 1, (b), (c) and (d). The distance traveled in the radar beam and the time available for acquisition are included in Figures 17 and 18 for these trajectories.

The interval detection probability for trajectory (b) is given in Figure 20. Similarly, the interval detection probability for trajectories (c) and (d) are given in Figures 21 and 22.

As indicated by the interval detection probabilities, the integrated detection probability rises rapidly to a value approximating 100 per cent for all ship positions between 600 and 1,000 nautical miles from the re-entry point.

The accumulated detection probability is plotted as a function of the distance from the tracking station in Figure 23. This indicates that a module, approaching a tracking station along any of the normal trajectories would be subject to a 99.5 percent detection probability at a range of 200 miles or more from the station. This would apply to any station location between 600 and 1,000 nautical miles from the re-entry point. It does not mean that all station positions have equal detection probabilities, however. An examination of the interval detection probability curves shows that a station located at about 850 nautical miles from the re-entry point will have more 99.9 percent detection intervals for more types of trajectories than other station locations.

VI. CONCLUSIONS

The analysis indicates that a radar which is capable of meeting the specified detection performance will entertain a high probability of success against the Command Module in the re-entry phase.

As far as detection probability is concerned, a ship or station location 850 nautical miles down range would be most suitable.

However, there are some other features which should be considered in the selection of a station position. Precursor attenuation, as shown in Figure 7, suggests that the station should be more than 650 nautical miles from the re-entry point.

The time available for data reception is also an important consideration for station location. As shown in Figure 24, time for data increases as the station is moved down range (this is true in all but the short trajectories where the data time is limited by the time between the end of the first data blackout and the initiation of the second data blackout). This feature suggests moving the station down range as far as possible.

Errors in the ship position, or in establishing the position of the re-entry point tend to increase the lateral displacement along the trajectory. Similar excessive lateral distance could result from trajectories with excessive acceleration forces. These features favor moving the station up range to a position where lateral range cannot cause non-detection.

When these factors are taken into consideration, the station location at 850 nautical miles from the re-entry point appears to be a good choice.

Other design considerations should include the following operational conditions:

(a) For any station location less than 1,000 nautical miles down range, the initial blackout of the S-Band data equipment extends to, or beyond, the station (see trajectory curves, Figures 1 through 5). This means that the radar will have to track the module from acquisition to some point down range from the station. The radar should be capable of continuous tracking at or near the zenith. Also, after the module has passed the station, the angular resolution should be good enough to place the S-Band data equipment on the target at the termination of the blackout.

(b) An examination of the aspect angle curves, Figures 13 and 14, and the target size curve, Figure 10 shows that after zenith the target size may be 0.2 square meters. The range capability of the radar on this size target will be reduced to 187 miles. It is desirable that blackout be terminated before this range is exceeded or some difficulty may be experienced in transfer from radar to S-Band tracking.

(c) In reporting on the Marchetti pulse radar track of the MA-6 Mercury capsule⁷ by Lin, Goldberg and Janney, it was disclosed that as many as five echoes were received near the end of the trajectory. The extra targets were attributed to particles which had become detached from the module and were forming their own ionization ball. Some consideration should be given to resolving the correct target in a possible situation of this kind during the Apollo re-entry.

ACKNOWLEDGMENTS

The author wishes to thank Dr. F. O. Vonbun for suggestions and recommendations incorporated in the report and for reviewing the completed manuscript. The assistance of Mr. R. E. Coady and Mr. T. E. Jones in the preparation of trajectory material is appreciated.

REFERENCES

1. Vonbun, F. O. "Re-Entry Tracking for Apollo" GSFC, March 1964.
2. Vonbun, F. O., "Apollo Re-Entry Infrared Support" GSFC, December 5, 1964.
3. Chapman, D. R., "An Approximate Analytical Method for Studying Entry Into Planetary Atmospheres," Ames Research Center, 1959.
4. Bryant, J. P. and Frank, M. P., "An Automatic Long Range Guidance System for a Vehicle Entering at Parabolic Velocity," Martin Company, June 1962.
5. Lehnert, Richard and Rosenbaum, Bernard, "Plasma Effects on Apollo Re-Entry Communications," NASA Technical Note D-2732, March 1965.
6. Daniels, R. L., "Final Report on Apollo Plasma Re-Entry Studies," North American Aviation Inc., SID 63-746 July 5, 1963.
7. Lin, S. C., Goldberg, W. P. and Janney, R. B., "Radio Echoes from the Ionized Trails Generated by a Manned Satellite during Re-Entry," AVCO Everett Research Report 127, April 1962.
8. Nolen, J. C., Lacis, J. G., and Smith, J. J., "Sequential Detection with Application to Radar," February 14, 1964.

TABLE I
Target Performance Trajectory

Station Distance from Re-Entry Point (n. mi.)	Forward Visibility Distance of Beam (n. mi.)	Distance in Radar Beam (n. mi.)	Average Velocity in Radar Beam (n.mi./sec.)	Available Acquisition Time (sec.)	Number of Five Second Search Frames	Distance Visible After Blackout (n. mi.)	Average Velocity After Blackout (n.mi./sec.)	Time for Data After Blackout (sec.)
(a) D = 5,000 nautical miles L/D = 0.4 $\gamma = 6.0^\circ$ Target = 1 sq. meter								
600	338	120	5.51	21.8	4.35	324	3.80	85.3
700	286	130	5.11	25.4	5.08	446	3.80	117.4
800	276	118	4.51	26.2	5.23	560	3.80	147.4
900	282	117	4.10	28.5	5.71	675	3.80	177.6
1,000	295	88	3.86	22.8	4.56	805	3.80	211.8
1,100	312	36	3.82	9.4	1.88	935	3.80	246.1
(b) D = 1,500 nautical miles L/D = 0.14 $\gamma = -6.0^\circ$ Target = 1 sq. meter								
600	338	120	5.51	21.8	4.35	215	3.20	67.2
700	286	132	5.09	25.9	5.19	304	3.10	98.1
800	276	127	4.42	28.7	5.75	388	3.00	129.3
900	270	114	3.88	29.4	5.88	430	2.90	148.3
1,000	274	74	3.54	20.9	4.18	430	2.90	148.3
1,100	293	22	3.48	6.3	1.26	430	2.90	148.3
(c) D = 2,000 nautical miles L/D = 0.4 $\gamma = -7.51^\circ$ Target = 1 sq. meter								
600	270	118	4.57	25.8	5.16	537	3.57	150.0
700	265	102	3.94	25.9	5.18	615	3.57	172.0
800	281	103	3.71	27.8	5.55	698	3.57	195.0
900	306	88	3.60	24.4	4.89	776	3.57	217.0
1,000	332	72	3.57	20.2	4.04	846	3.57	237.0
1,100	350	63	3.56	17.7	3.54	910	3.57	255.0
(d) D = 2,000 nautical miles L/D = 0.4 $\gamma = 5.53^\circ$ Target = 1 sq. meter								
600	370	103	5.61	18.4	3.67	36	3.65	10.0
700	316	114	5.42	21.0	4.20	125	3.40	37.0
800	295	121	5.06	23.9	4.78	210	3.30	64.0
900	290	120	4.68	25.6	5.13	290	3.30	88.0
1,000	288	116	4.34	26.7	5.34	360	3.30	109.0
1,100	287	85	4.18	20.3	4.61	420	3.30	127.0

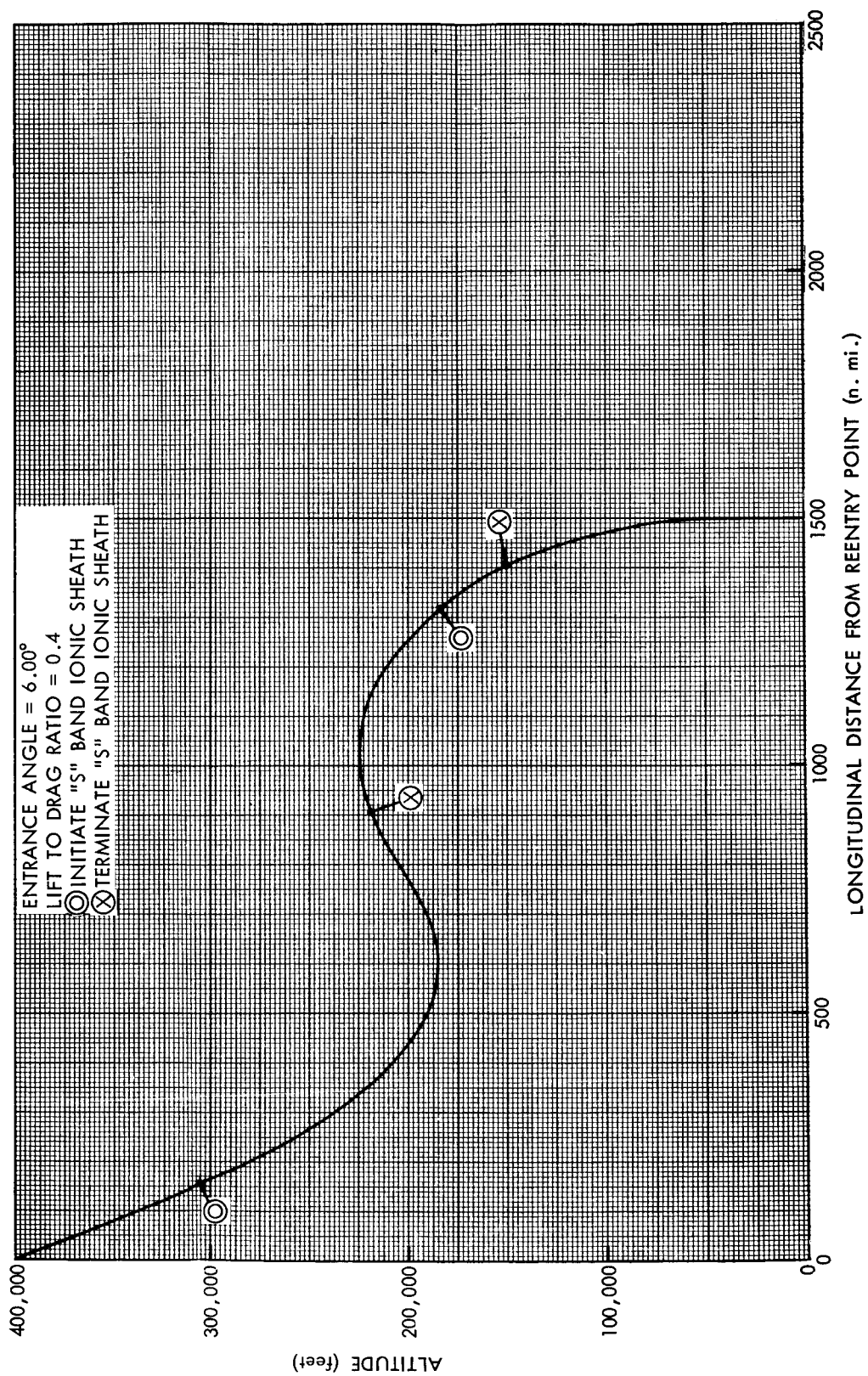


Figure 1—Vertical Projection, 1500 Nautical Miles Trajectory

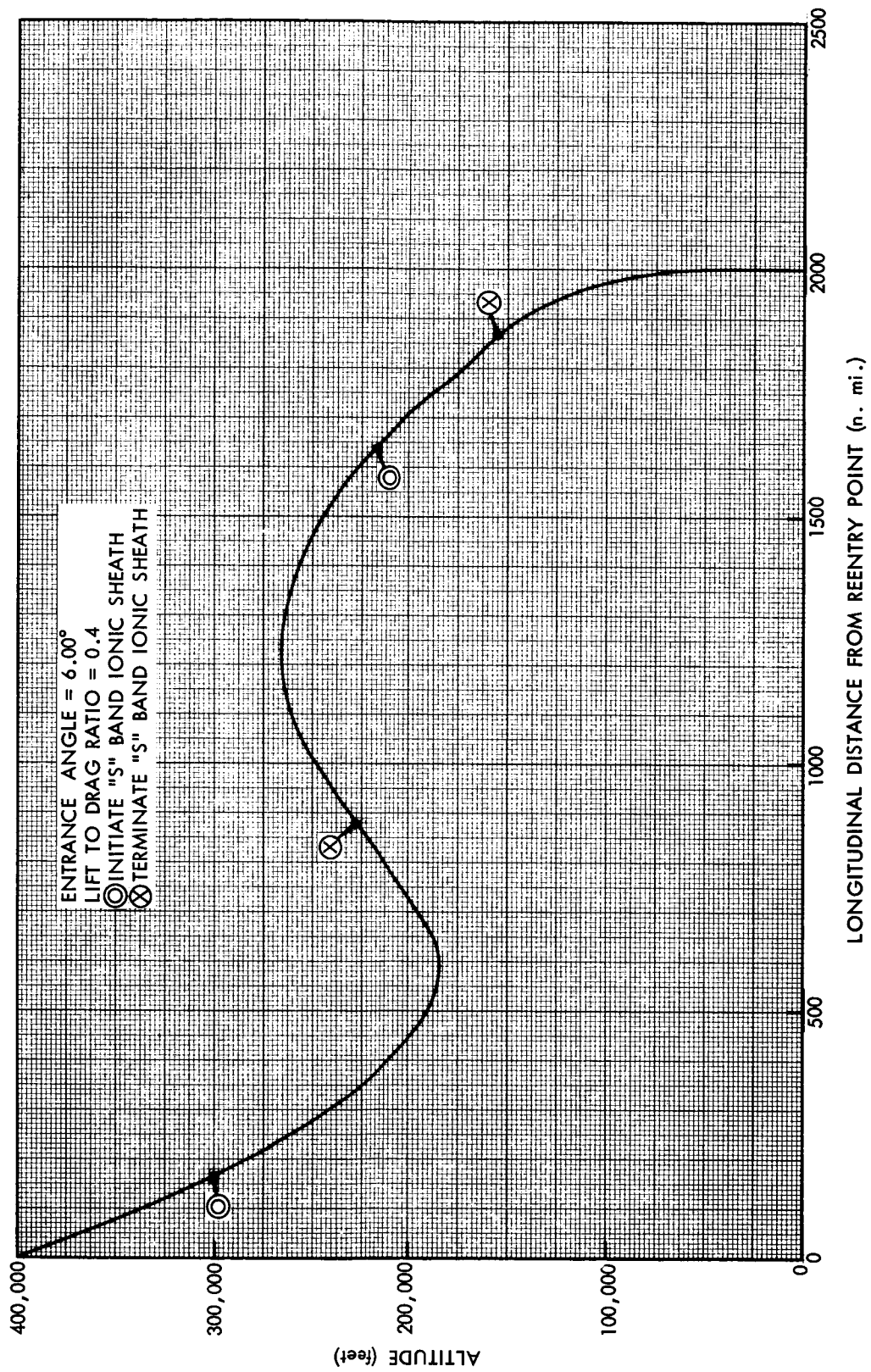


Figure 2—Vertical Projection, 2000 Nautical Miles Trajectory

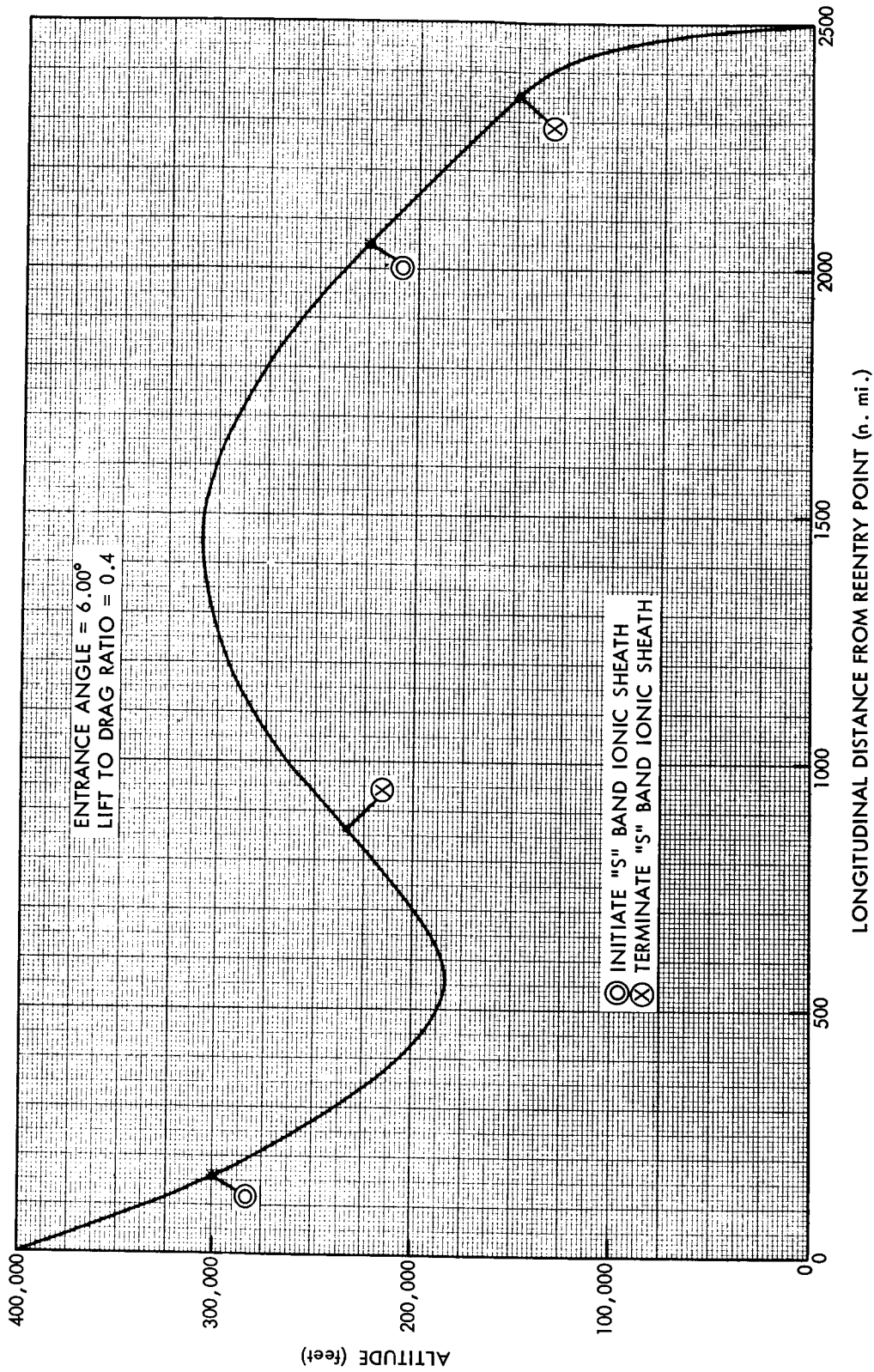


Figure 3—Vertical Projection, 2500 Nautical Miles Trajectory

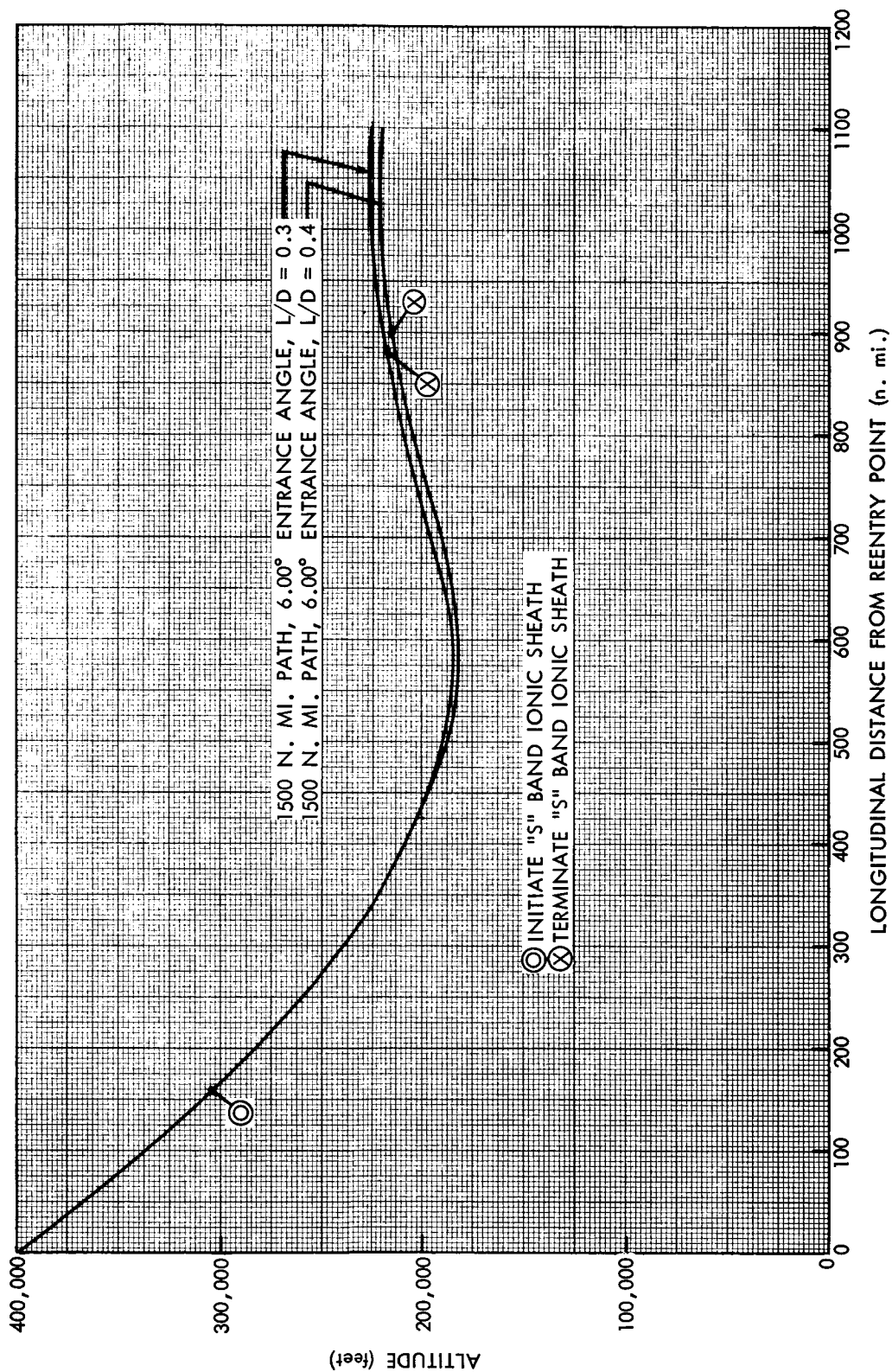


Figure 4—Vertical Projection, 1500 Nautical Miles Trajectory

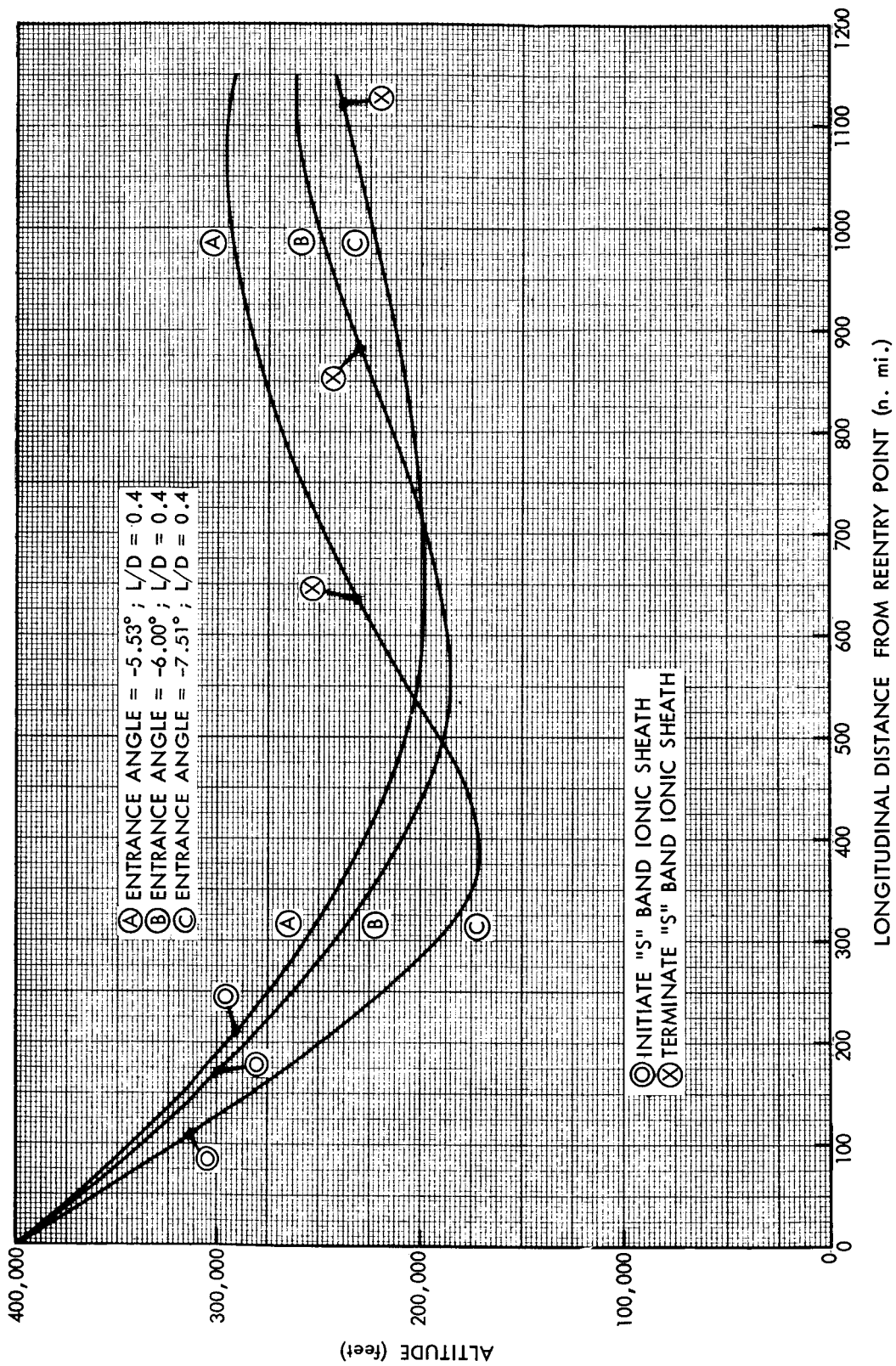


Figure 5-Vertical Projection, 2000 Nautical Miles Trajectory

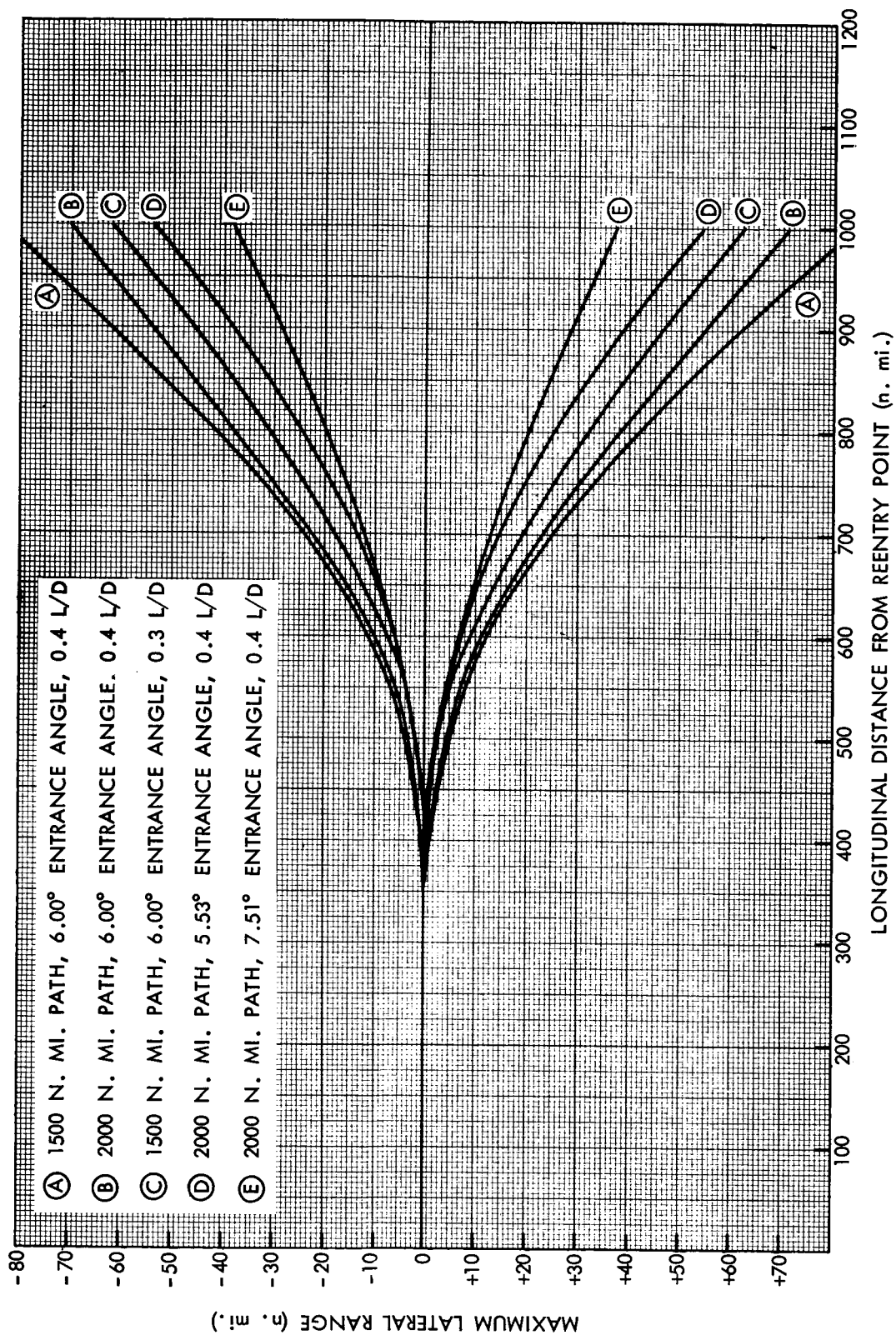


Figure 6—Maximum Lateral Range

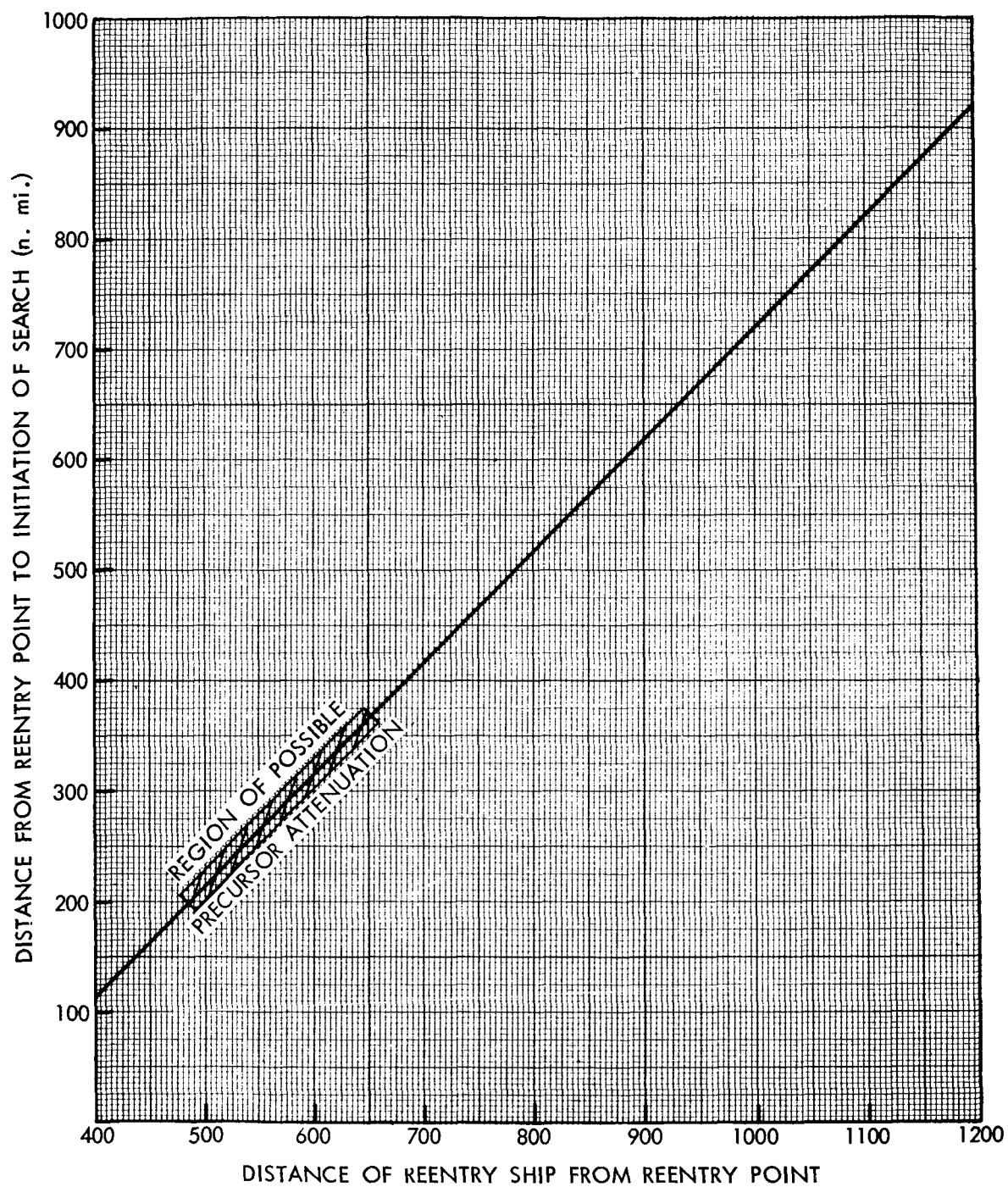


Figure 7—Precursor Attenuation Band

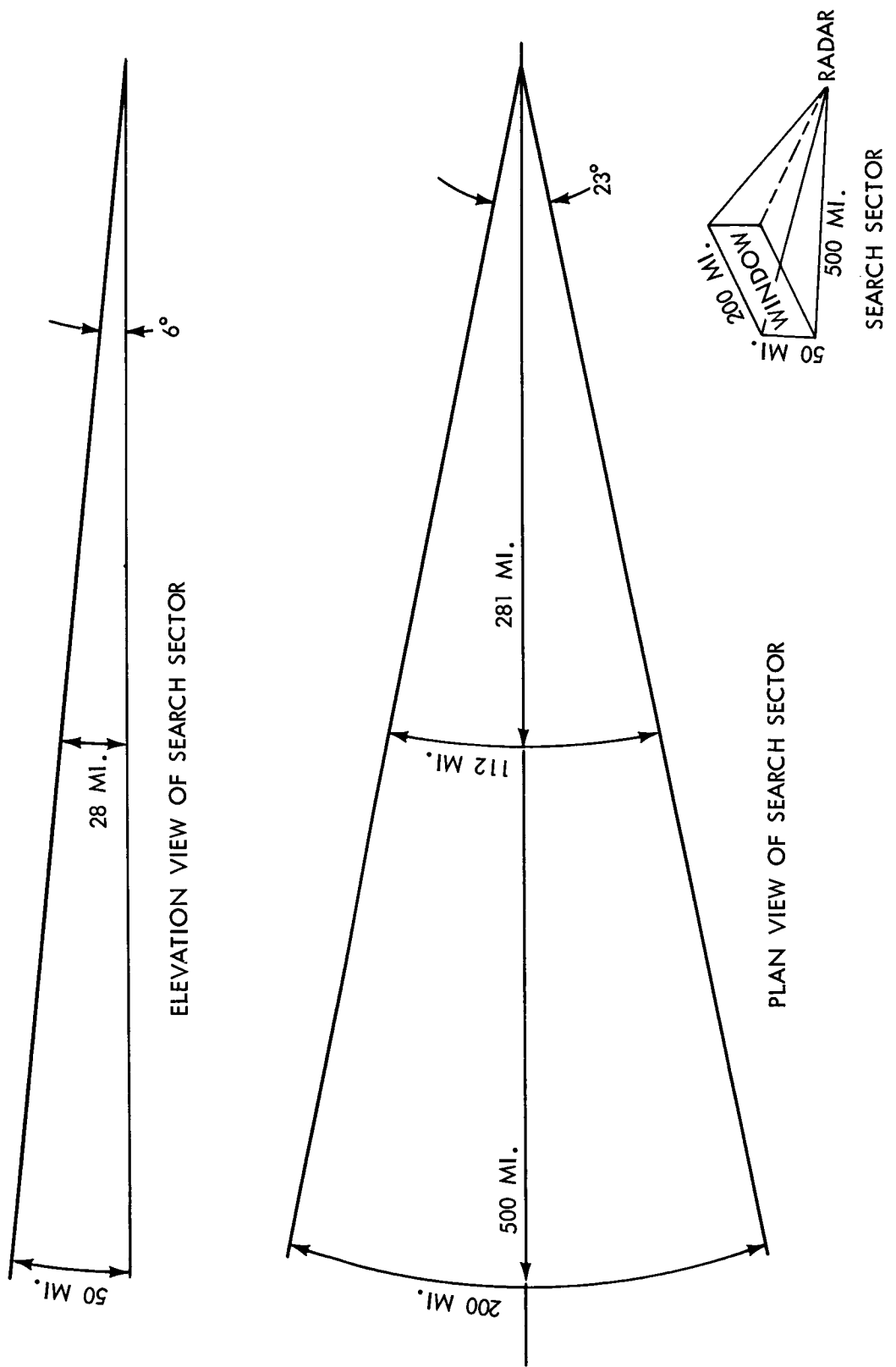


Figure 8—Proposed Search Sector

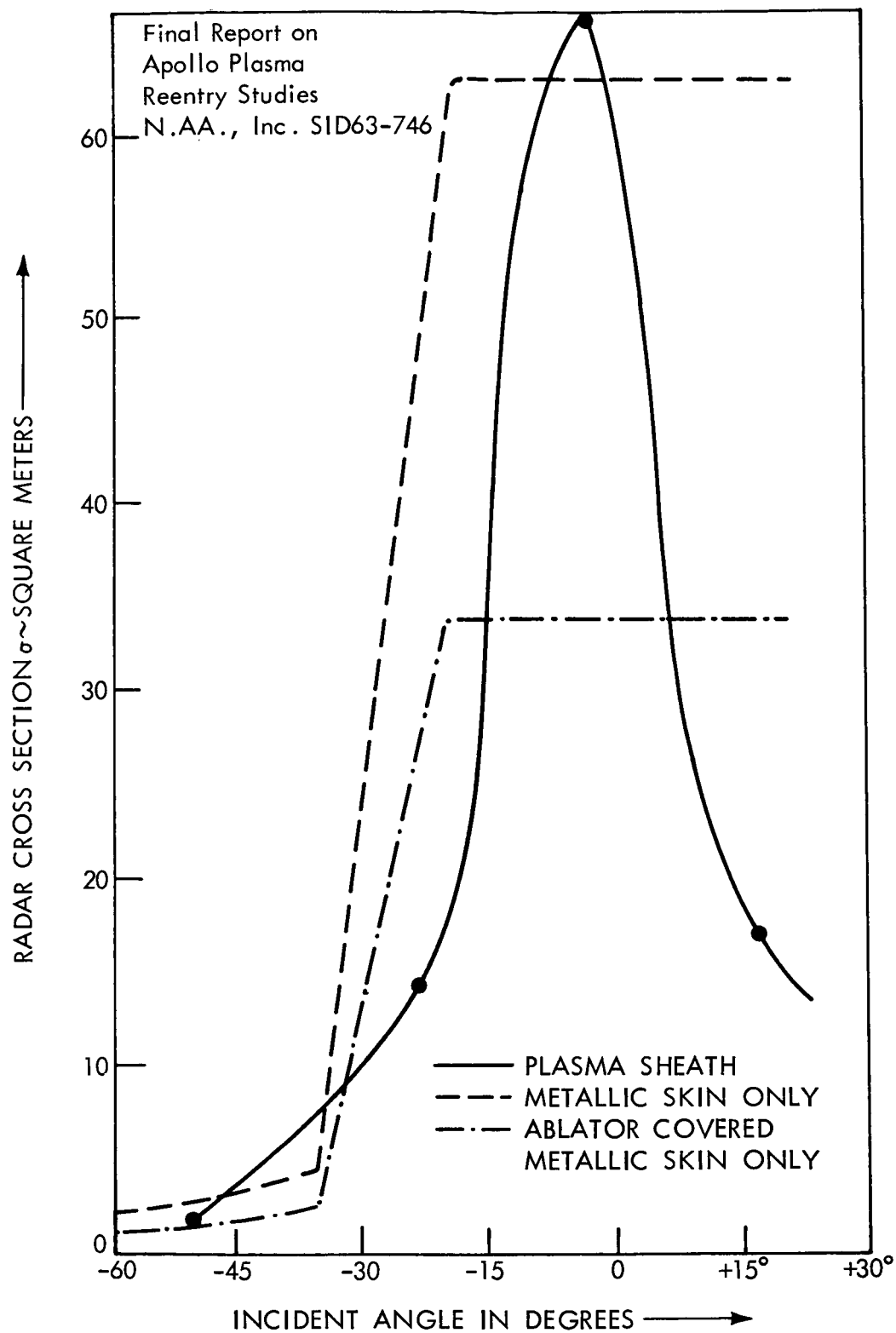


Figure 9—Radar Cross Section by North American Aviation

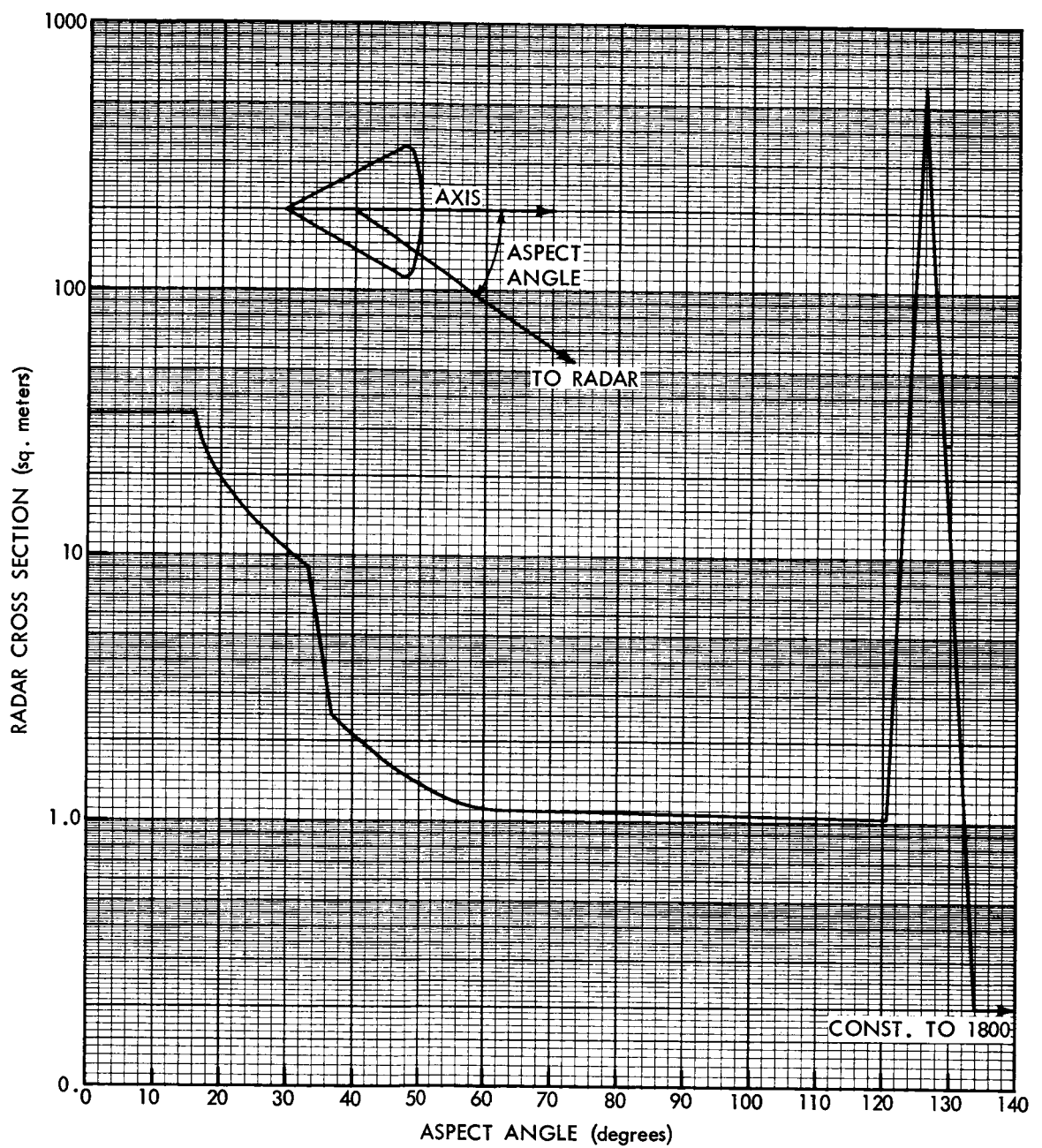


Figure 10—Radar Target Size

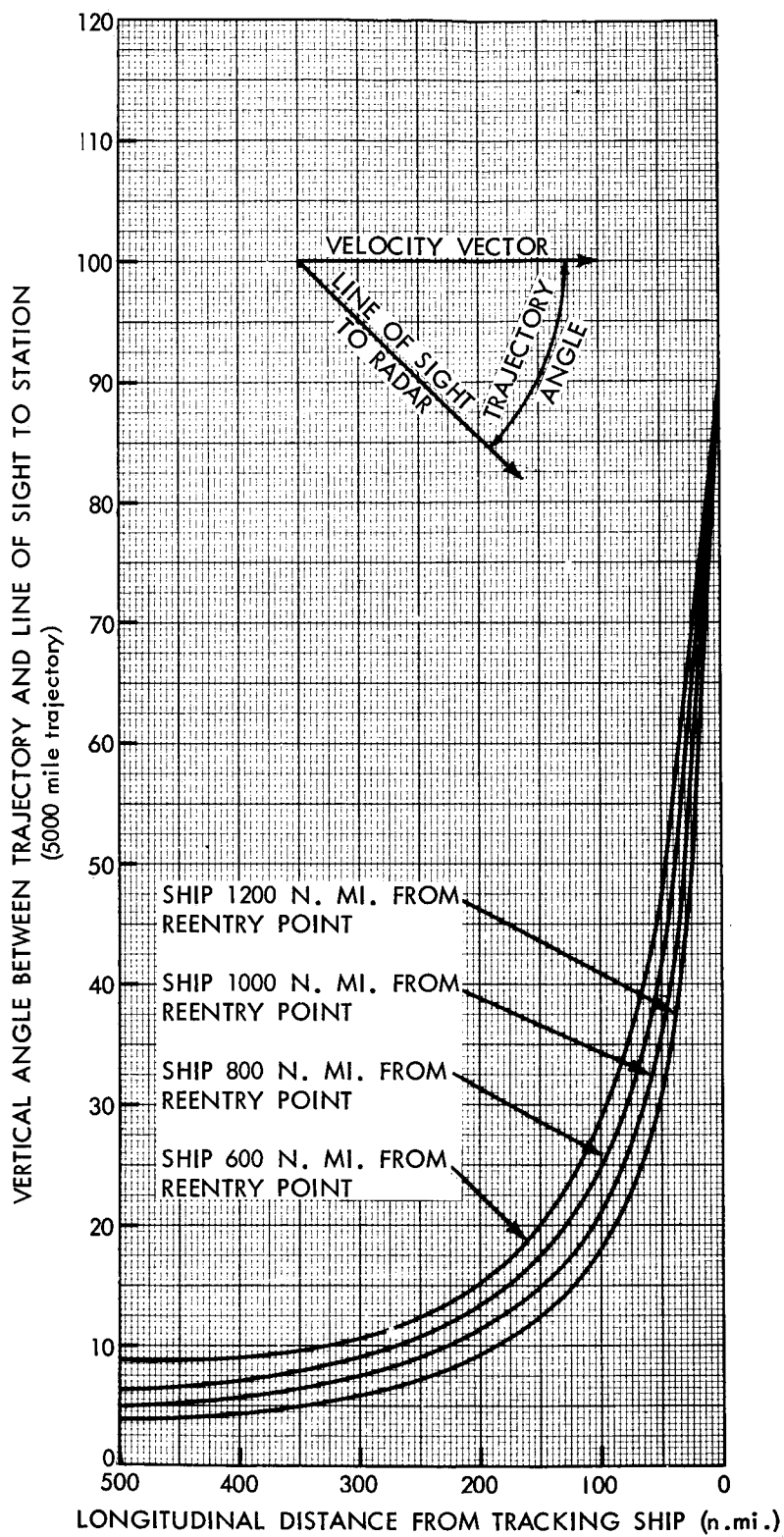


Figure 11—Vertical Trajectory Angles

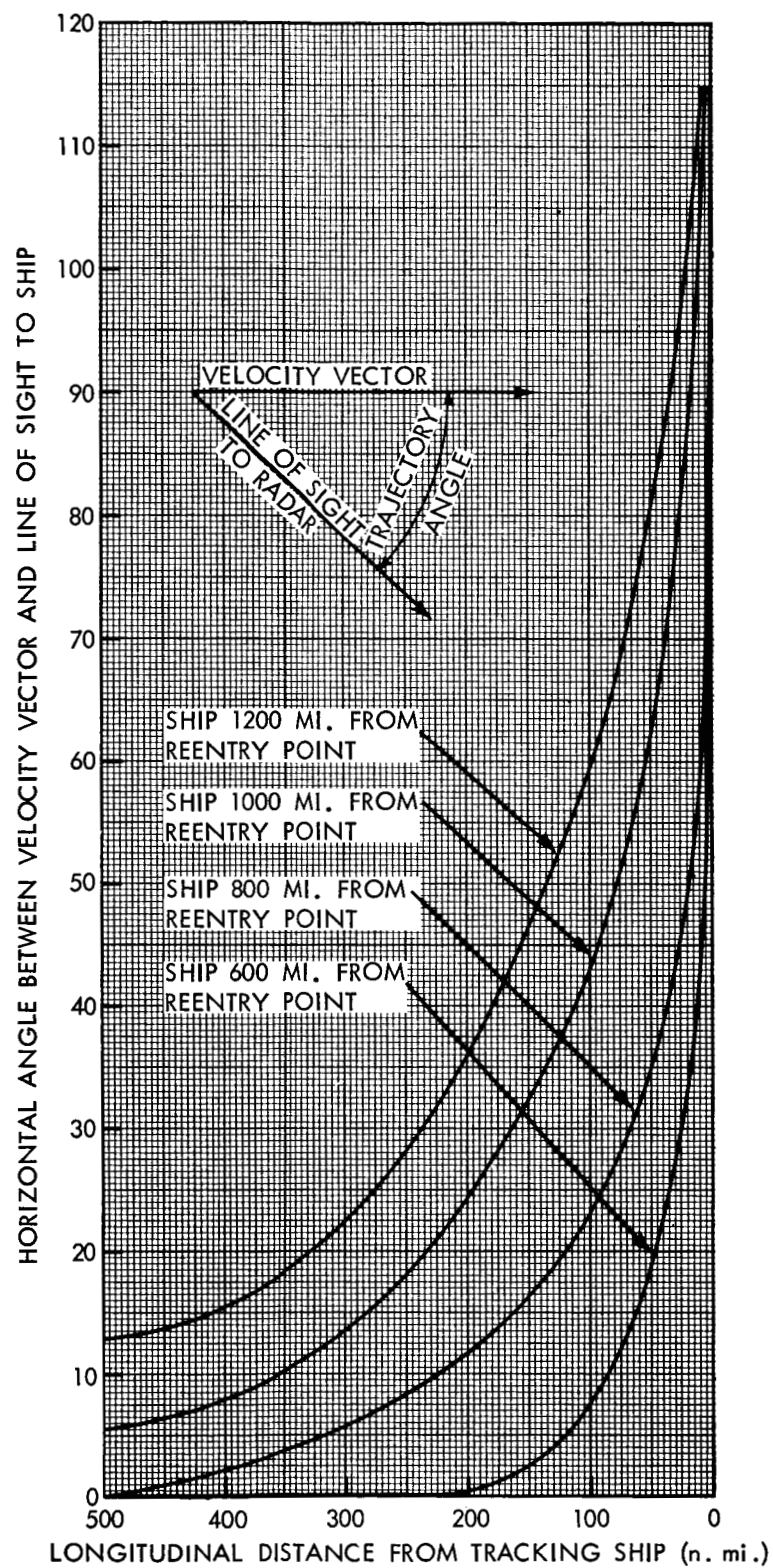


Figure 12-Horizontal Trajectory Angles

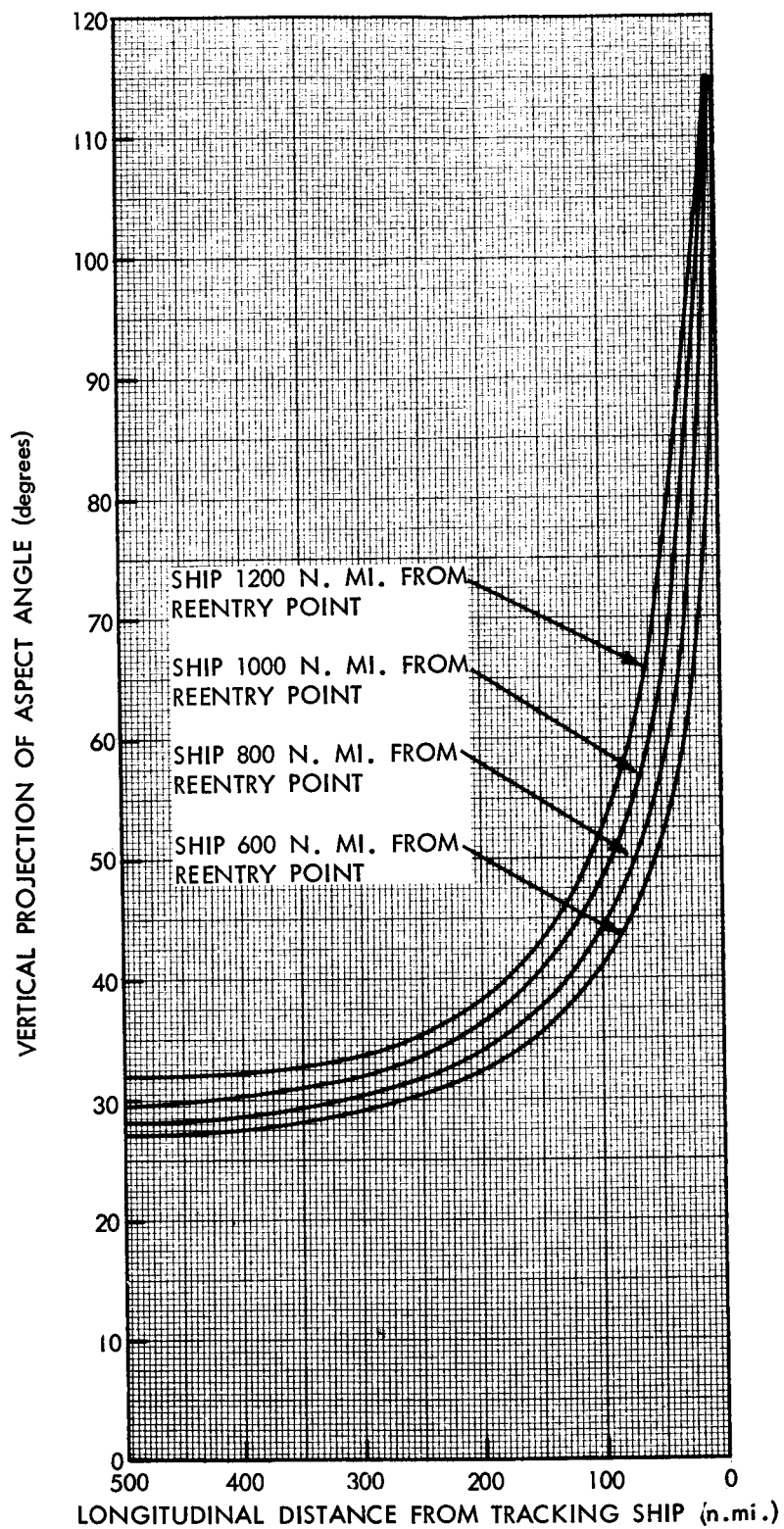


Figure 13—Vertical Projection of Aspect Angles

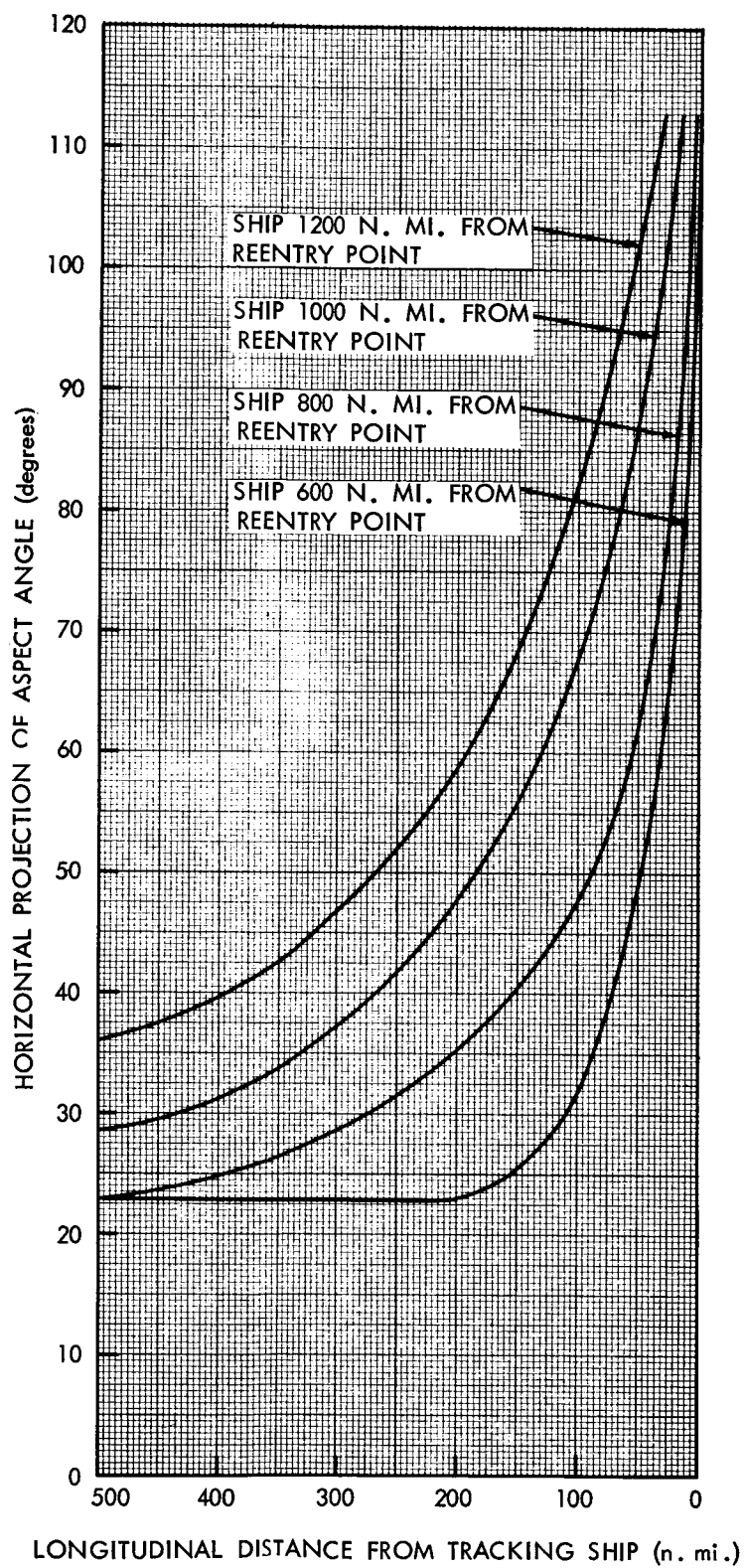


Figure 14—Horizontal Projection of Aspect Angles

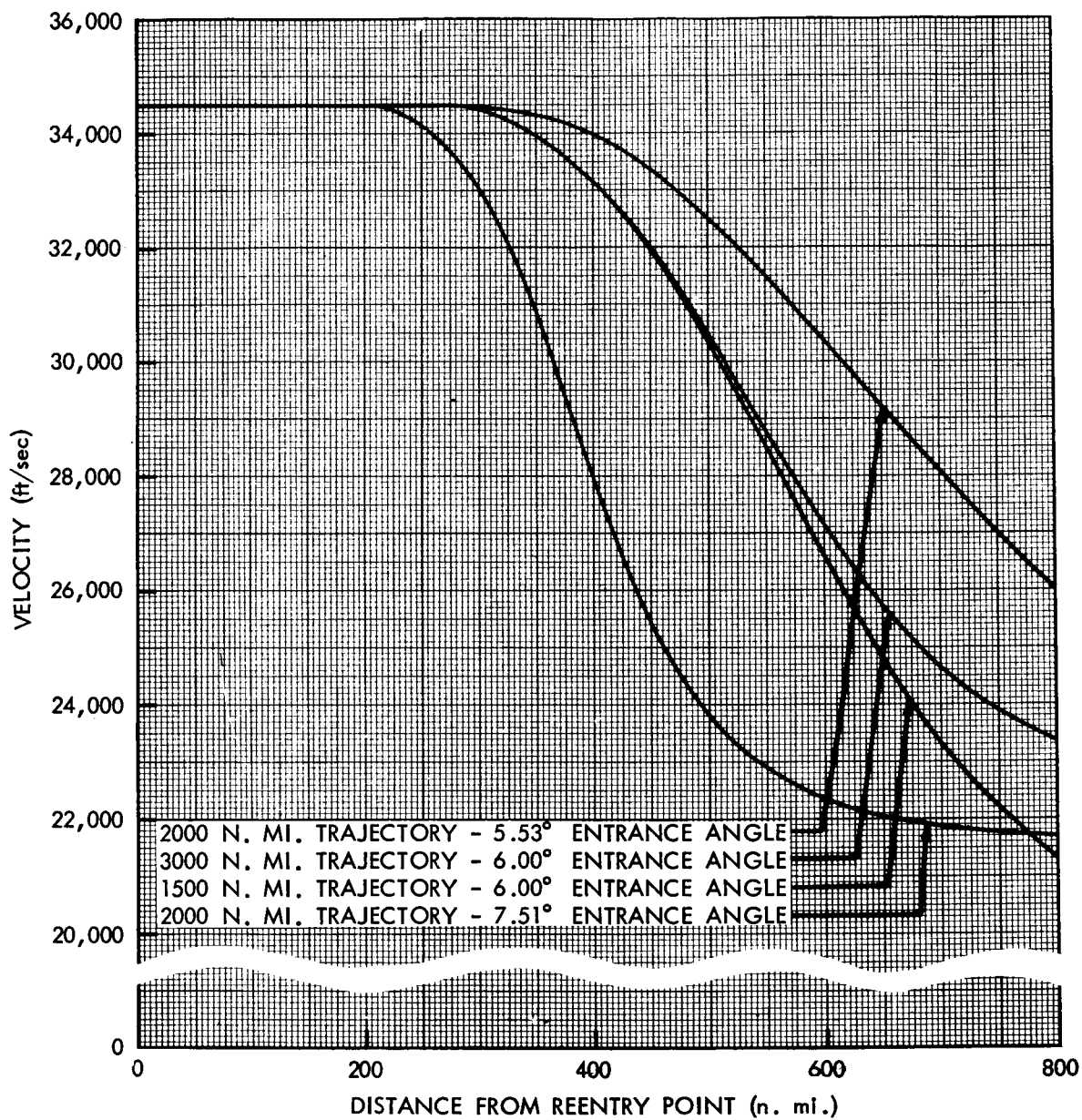


Figure 15—Module Velocity (feet per second)

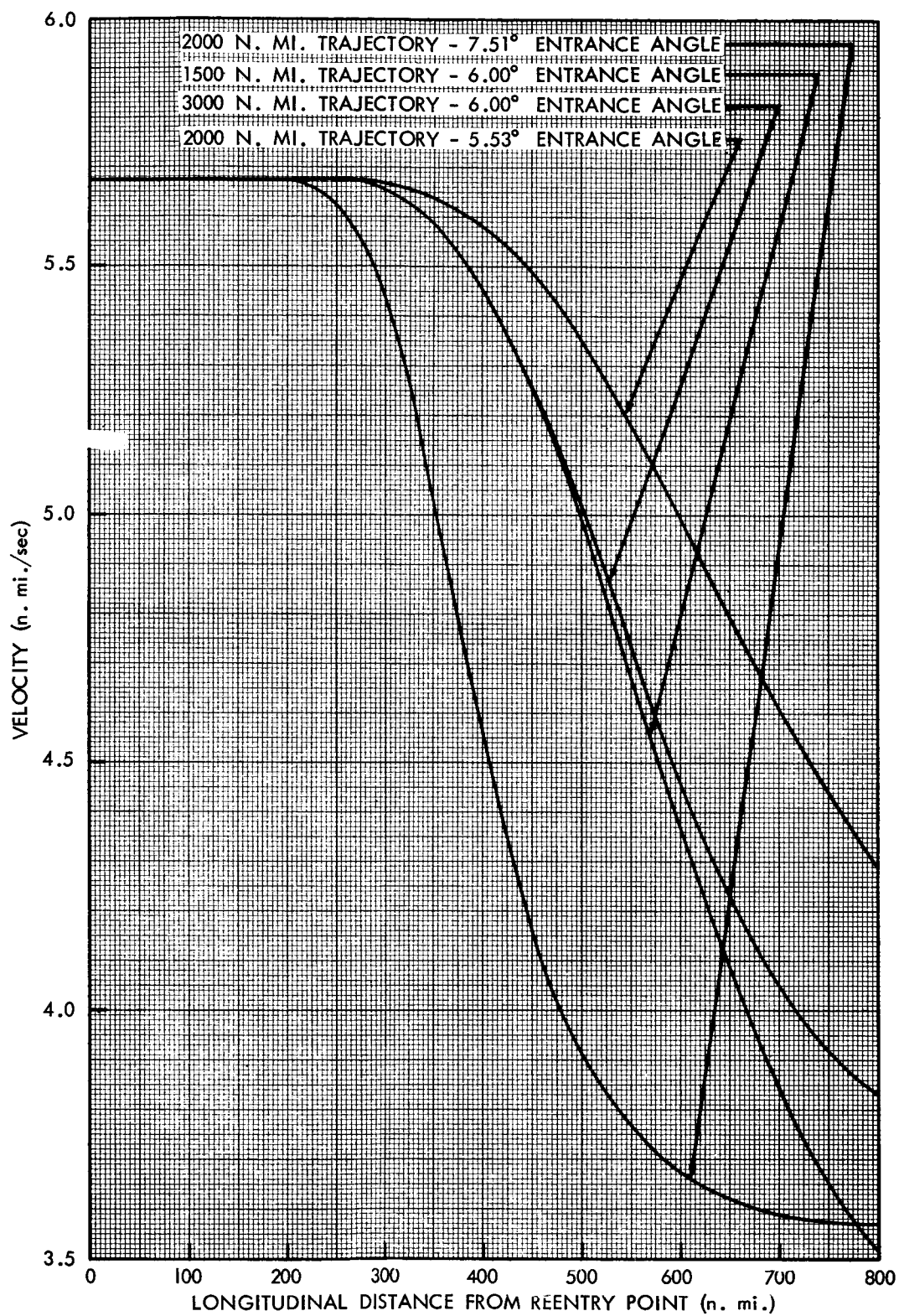


Figure 16-Module Velocity (nautical miles per second)

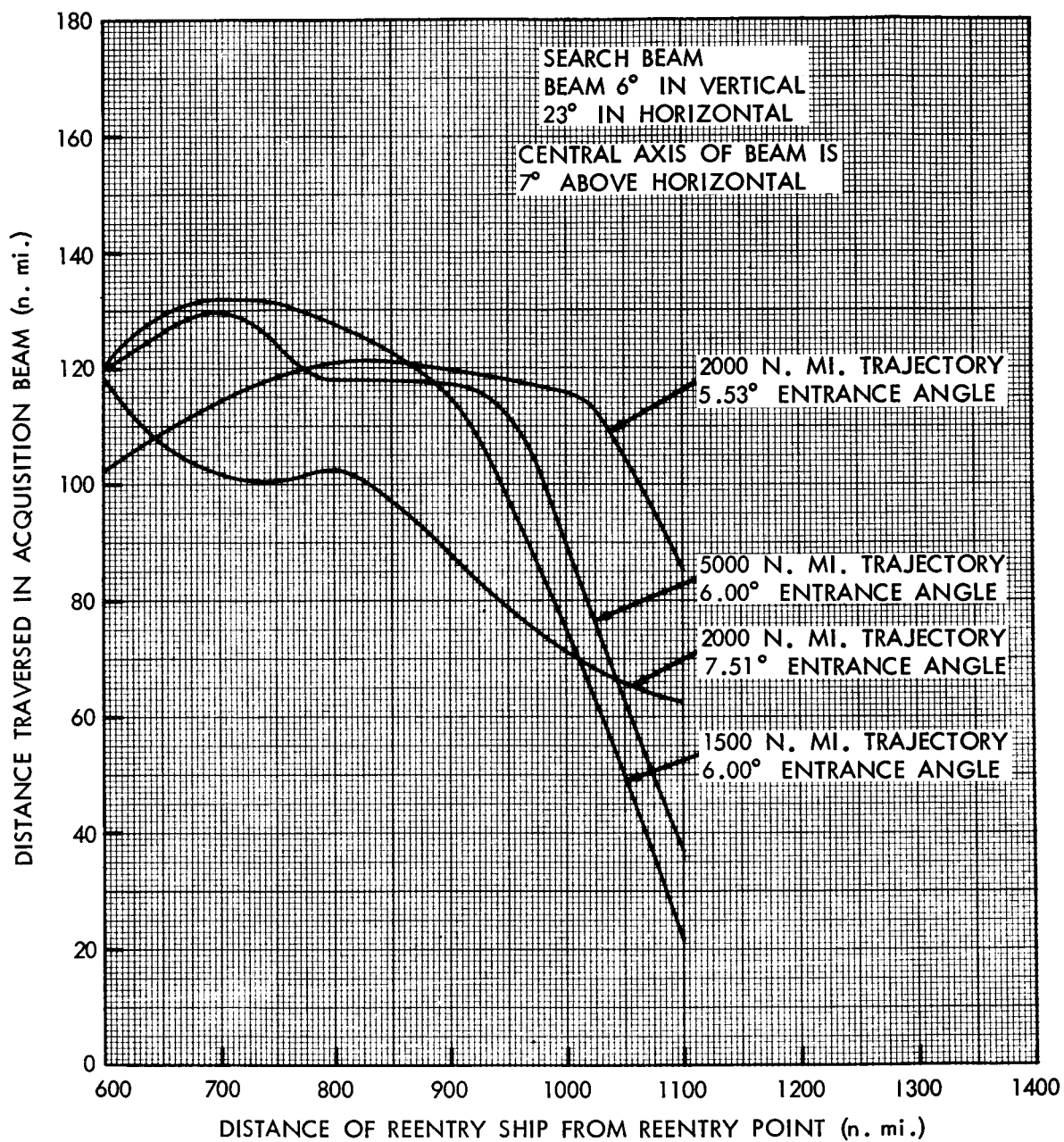


Figure 17—Distance Traveled in Acquisition Beam

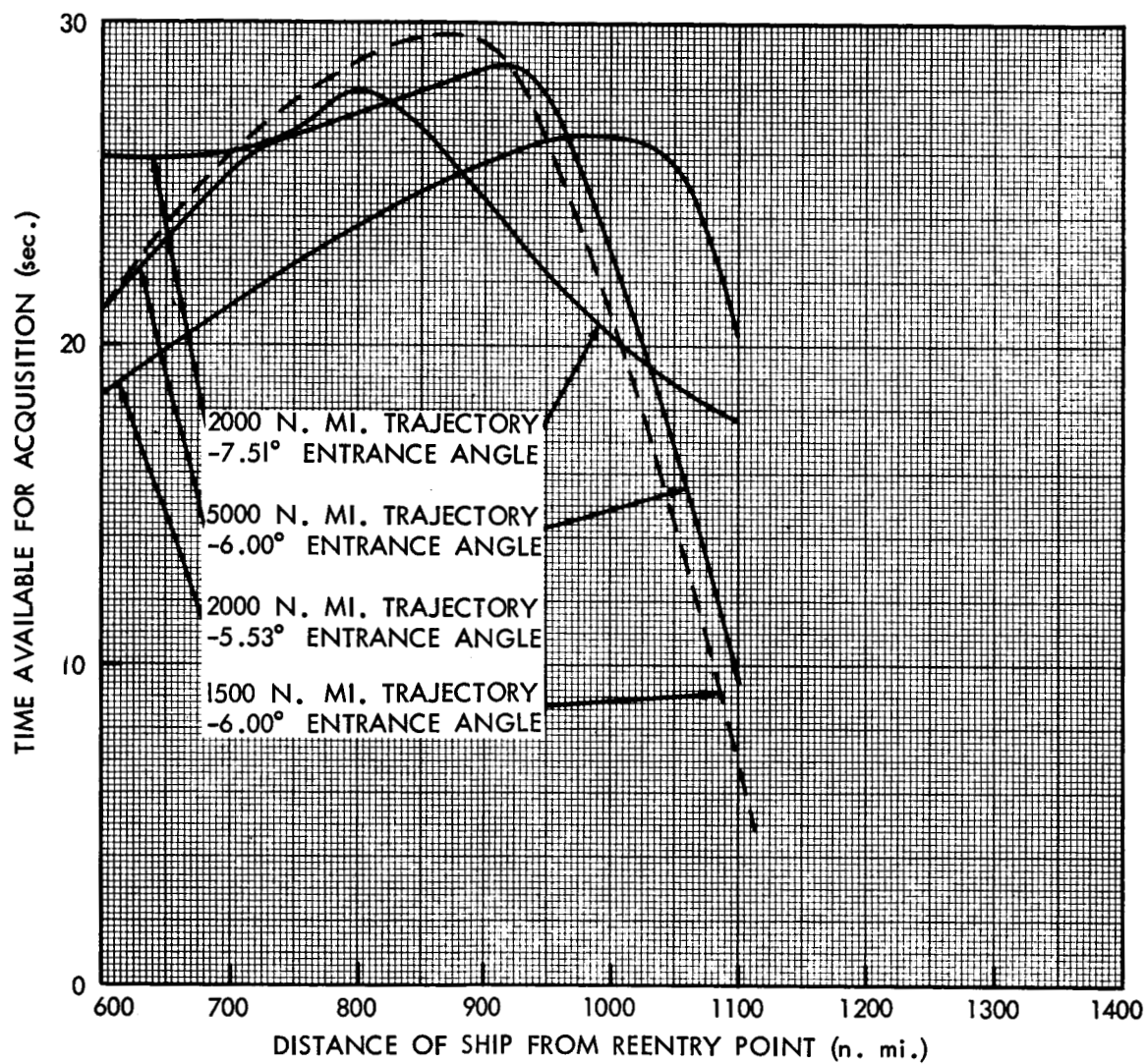


Figure 18—Time Available for Acquisition

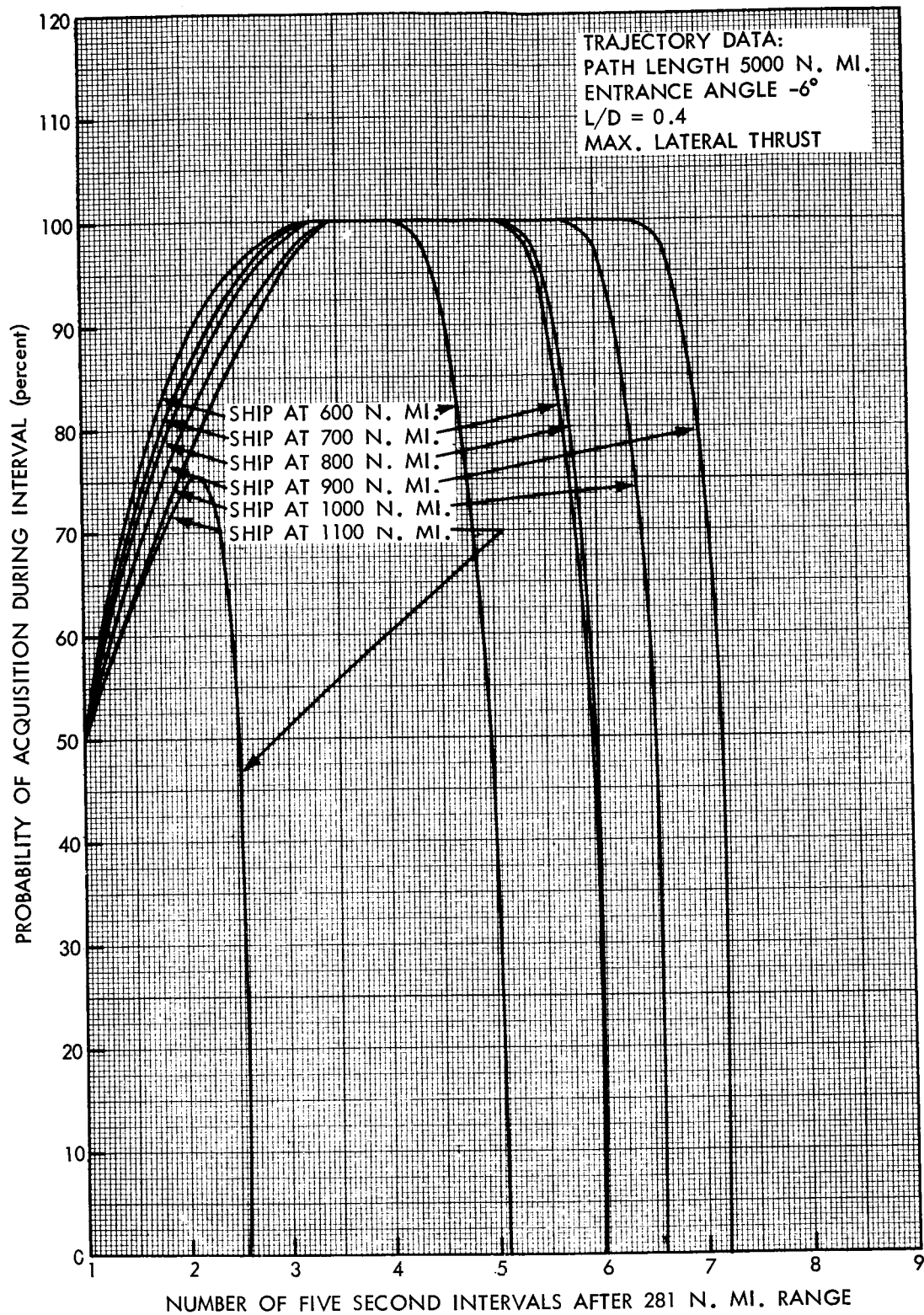


Figure 19—Interval Detection Probability, 5000 N. Mi. Trajectory

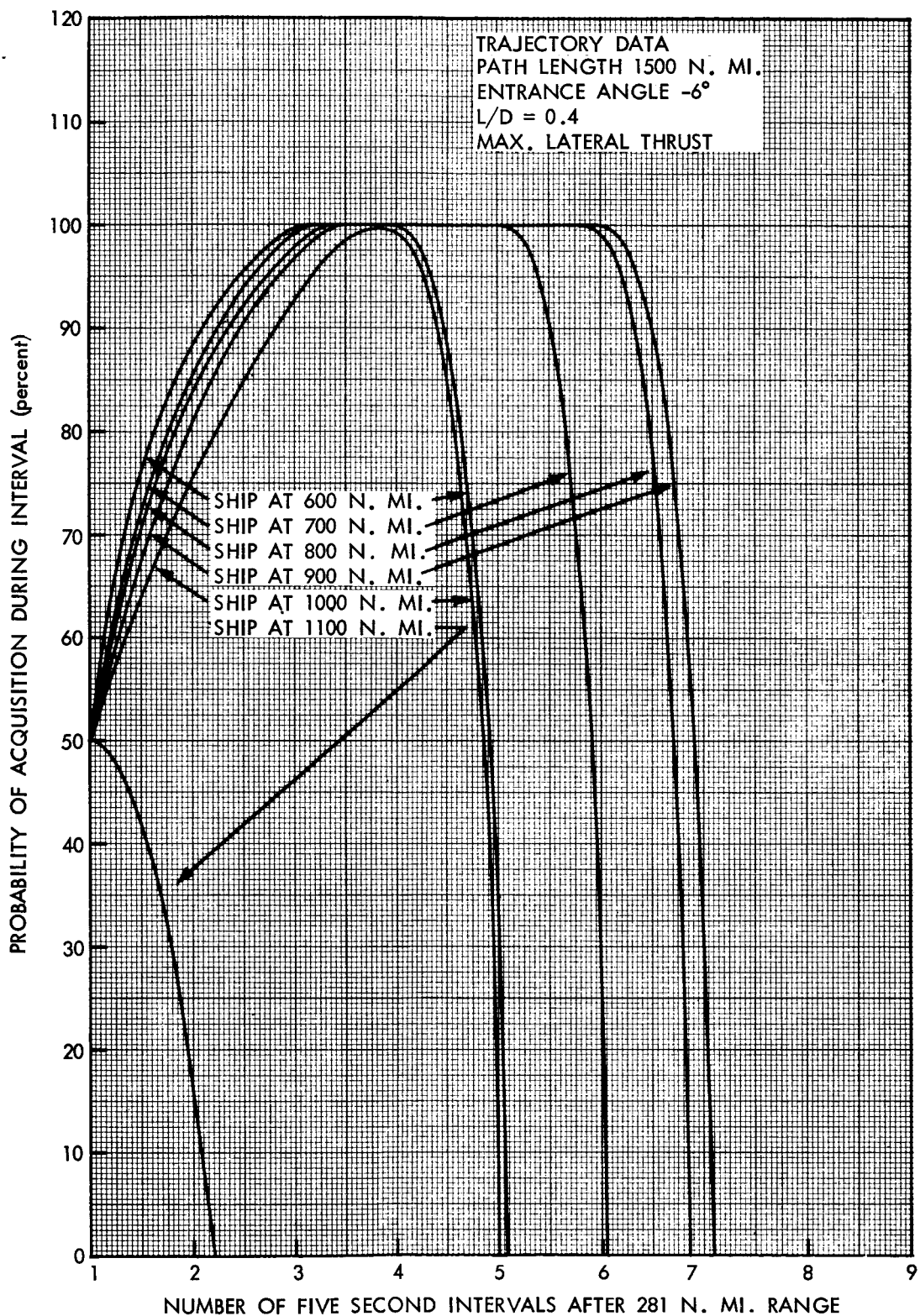


Figure 20—Interval Detection Probability, 1500 N. Mi. Trajectory

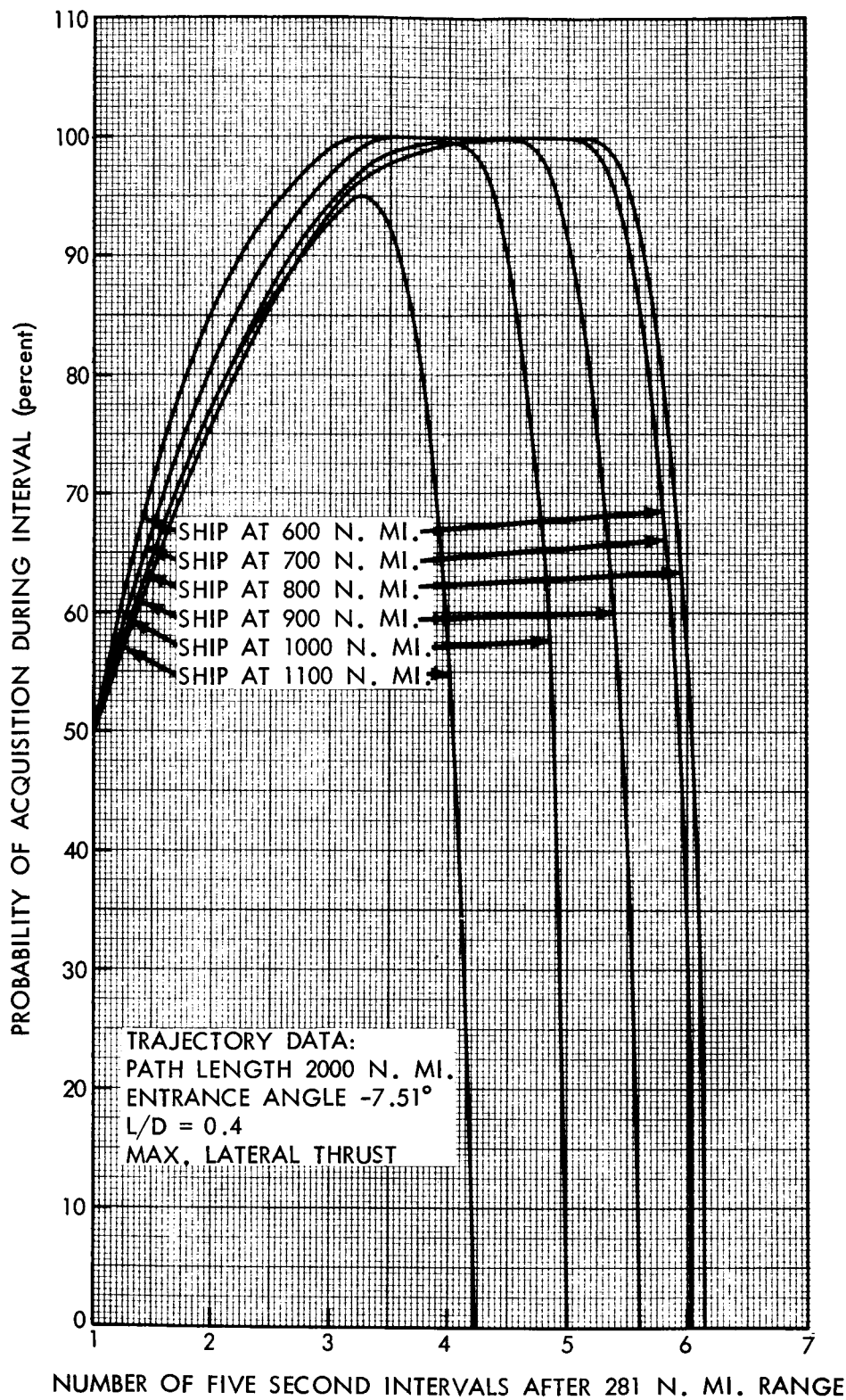


Figure 21—Interval Detection Probability, 2000 N. Mi. Trajectory

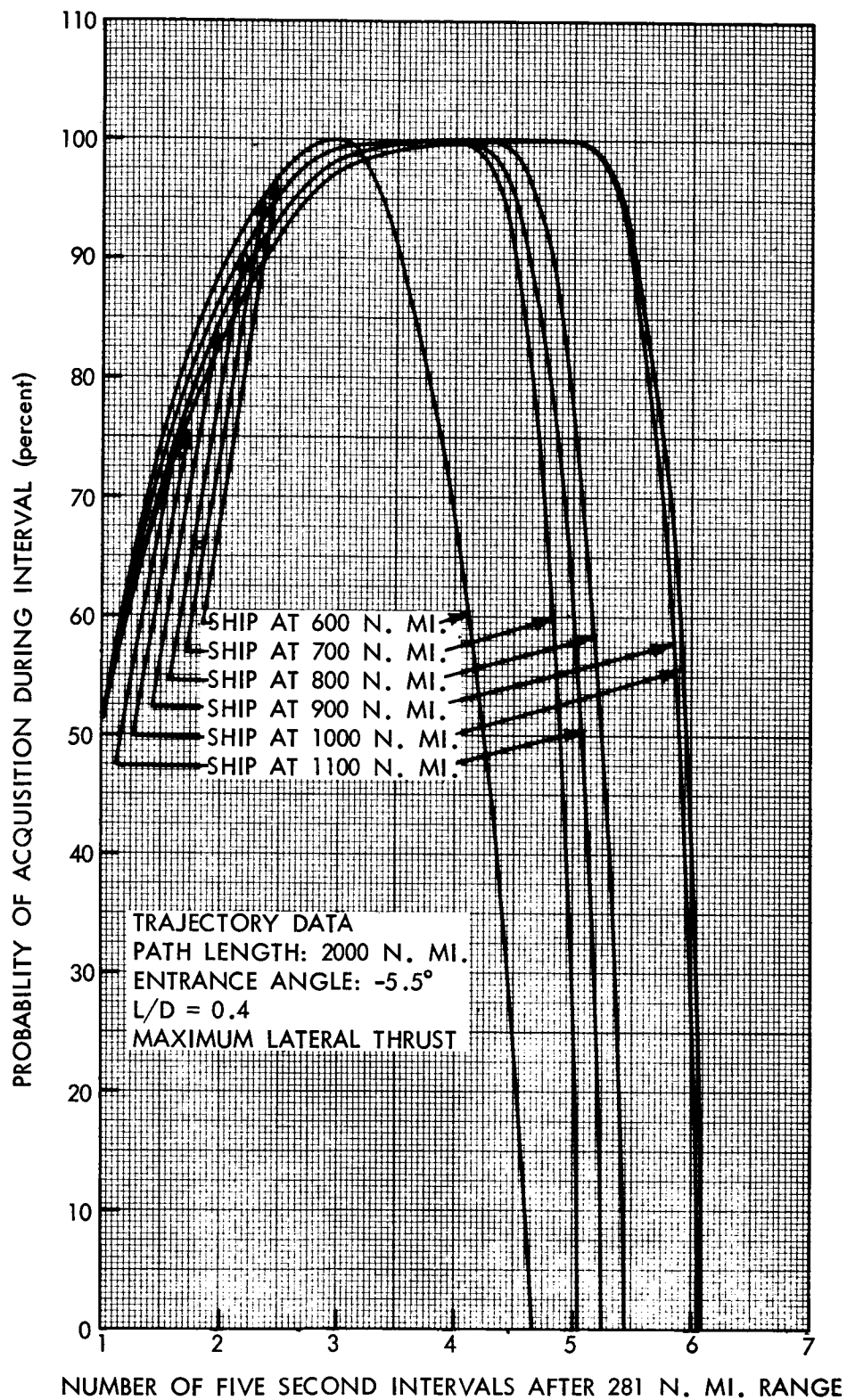


Figure 22—Interval Detection Probability, 2000 N. Mi. Trajectory

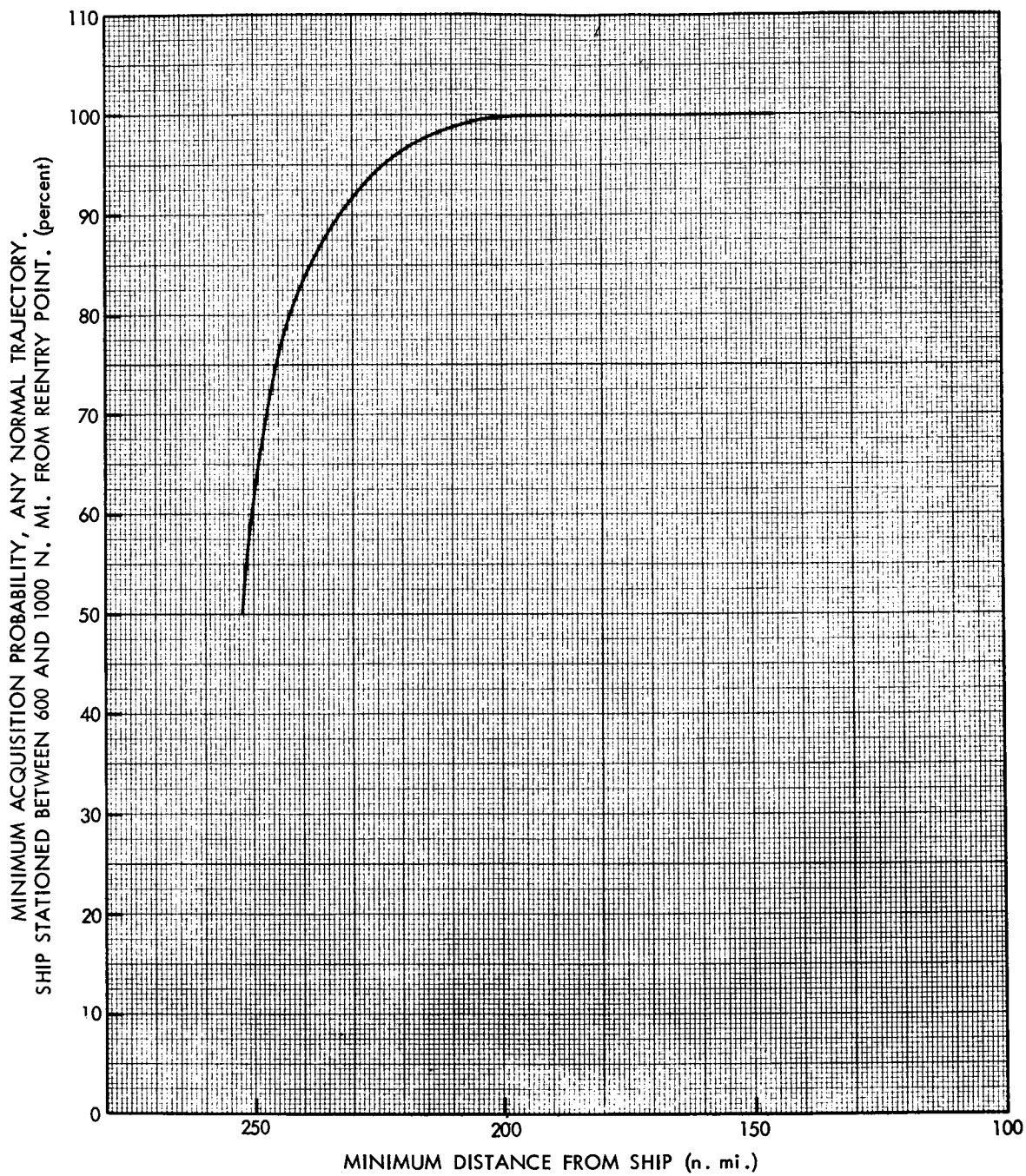


Figure 23—Accumulated Detection Probability

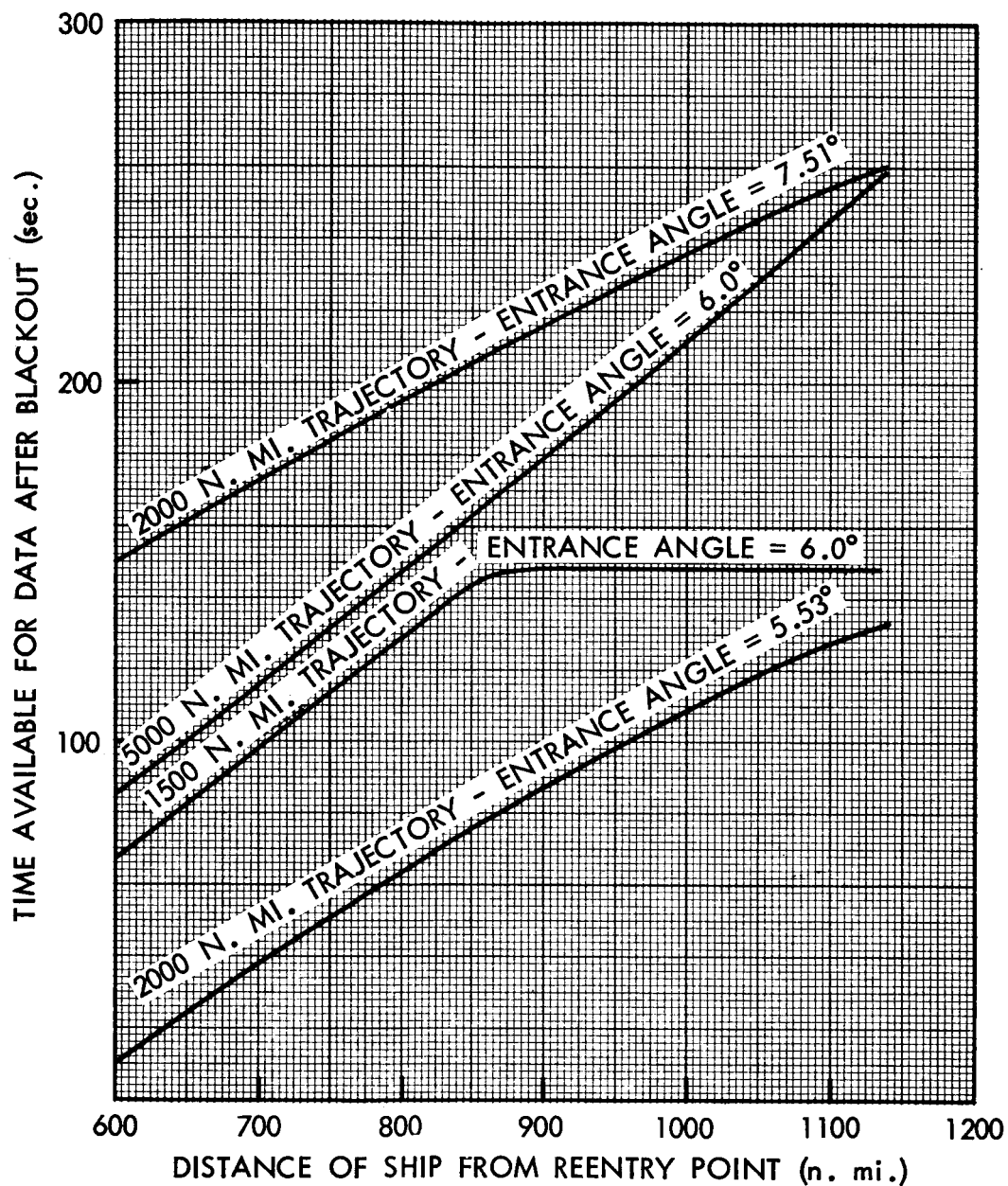


Figure 24—Time Available for Acquisition